Ab Initio study of structures and stabilities of substituted lead compounds. Why is inorganic lead chemistry dominated by PbII but organolead chemistry by PbIV?

ARTICLE *in* JOURNAL OF THE AMERICAN CHEMICAL SOCIETY · FEBRUARY 1993

Impact Factor: 12.11 · DOI: 10.1021/ja00056a034

Ab Initio Study of Structures and Stabilities of Substituted Lead Compounds. Why Is Inorganic Lead Chemistry Dominated by Pb^{II} but Organolead Chemistry by Pb^{IV}?

Martin Kaupp and Paul v. R. Schleyer*

Contribution from the Institut für Organische Chemie I, Friedrich-Alexander Universität Erlangen-Nürnberg, Henkestrasse 42, D-8520 Erlangen, Germany. *Received May 11, 1992*

Abstract: The influence of electronegative substituents on the structures and relative stabilities of lead(IV) versus lead(II) species has been assessed by ab initio pseudopotential computations for a series of halogenated lead hydrides and methyllead compounds R_nPbX_{4-n} (R = H, CH_3; X = F, Cl; n = 0–4) and R_nPbX_{2-n} (n = 0–2). The calculated energies of various model reactions reveal the drastic degree of destabilization of tetravalent lead compounds by electronegative substituents X (X = F, Cl). The bond angles in compounds with different groups, R_nPbX_{4-n} (n = 1–3), deviate widely from 109.5°. In agreement with Bent's rule, the angles between the most electronegative substituents (F or Cl) are smaller, while those between more electropositive groups (H, CH_3, SiH_3) are considerably larger than tetrahedral. The deformations computed for R_2PbX_2 and R_3PbX are related to those observed experimentally in various organolead and organotin structures. The destabilization of the tetravalent species by relativistic effects is larger when electronegative substituents are present. There also are large relativistic effects on bond angles (up to ca. 14°). All Pb–R and Pb–X bonds shorten upon successive substitution by electronegative groups; i.e., the weakening of the bonds is accompanied by a decrease of their lengths! A simple bonding model is proposed to explain both the thermodynamic and the structural observations: The increase of the positive metal charge upon halogen substitution results in greater contraction of the 6s-orbitals than the 6p-orbitals. Hence, the 6p-orbitals are less effective in sp^n hybridization, and electronegatively substituted Pb^{IV} compounds are destabilized. While the traditional term "inert pair effect" implies the energetic unavailability of a 6s-pair of electrons for bonding, the proposed concept emphasizes the size differences between s- and p-orbitals. This supports Kutzelnigg's analysis of the bonding in compounds of the heavy main group elements. A novel type of hyperconjugation, "geminal $\sigma PbH \rightarrow \sigma^*(PbH, PbF)$ hyperconjugation" also influences the relative stabilities of substituted lead(IV) compounds.

I. Introduction

Most of inorganic lead chemistry, e.g., the halides, oxides etc., is derived from Pb^{II}. In contrast, the inorganic Pb^{IV} compounds often are either unknown, are unstable transient species, or are highly reactive. The well-characterized inorganic Pb^{IV} species are strong oxidizing agents (e.g., PbO_2, $Pb(OAc)_4$).[1,2a] On the

0002-7863/93/1515-1061$04.00/0

other hand, organic lead compounds such as R_4Pb (R = alkyl, aryl) are relatively stable,[1,2] particularly in comparison with the corresponding divalent systems; R_2Pb compounds usually have only been postulated as unstable transient species (only a few exceptions are known[1-3]) The stability of mixed species R_nPbX_{4-m} where X is an electronegative substituent, decreases with decreasing n.[2] Thus, various monohalogenated and dihalogenated organolead derivatives are known, but trihalo species are elusive.[2] Similar differences between inorganic and organometallic thallium +I and +III chemistry are appreciated.[1,4a] While the higher oxidation states are less destabilized for the lighter elements, In and Sn, electronegative substituents also influence their chemistry similarly.[1,4b,c]

The instability of heavier group 13, 14, or 15 compounds exhibiting the maximum valency, compared to species with valencies reduced by two, is known as the "inert-pair effect".[5] Drago[6] criticized this term and rationalized the reduced valencies by an unfavorable balance between the bond energy gained in the higher valent compound and the promotion energy required to reach the higher valence configuration (e.g., sp^3 with PbX_4 compounds). Strong contributions from relativistic effects due to an increase of the sp-promotion gap from 5th to 6th period p-block elements also are well established.[7] However, we know of no conclusive explanation for the relative unimportance of the "inert-pair effect" in organolead chemistry and for the destabilization of organolead compounds by electronegative substituents.

These problems can now be investigated by means of ab initio quantum chemistry. In particular, pseudopotential methods facilitate ab initio calculations on compounds involving heavier elements[8] (density functional methods also are very promising[9]). The major relativistic effects[7] can be included conveniently by fitting the atomic pseudopotential parameters to relativistic or quasirelativistic all-electron data.[8] The comparison of calculations with relativistically and nonrelativistically adjusted pseudopotentials allows the straightforward identification of the influence of relativistic effects on molecular properties.[7] Indeed, Schwerdtfeger et al. have recently analyzed the differences between organothallium and inorganic thallium chemistry by relativistic pseudopotential calculations.[10] They argued that the destabilization of monovalent organothallium species RTl by spin–orbit coupling may contribute to the stability of Tl(III) in organometallic systems. While they also postulated that charge transfer from the Tl 6s-orbital to electronegative ligands might be a destabilizing factor, no data in support of this idea were provided. During the course of our own work, Schwerdtfeger et al. reported extensive ab initio pseudopotential calculations on heavy main group hydrides and halides including those of Tl and Pb.[11] The authors noted that, e.g., the average Pb–F bond dissociation energy (BDE) in PbF_4 is only ca. 80% of that in PbF_2. On the other hand, the average Pb–H BDE in PbH_4 is slightly larger than that in PbH_2.[11] In consequence, the disproportionation reaction $2PbX_2 \rightarrow PbX_4 + Pb$ is exothermic with X = H but strongly endothermic with X = F.

Table I. HF-Optimized Geometries of Halogenated Lead Hydrides[a]

	Pb–H	Pb–X	H–Pb–H	H–Pb–X	X–Pb–X
PbH_2	1.828		92.1		
	(1.854)		(92.7)		
PbHF	1.833	2.053		93.3	
	(1.854)	(2.022)		(92.6)	
PbF_2		2.027			95.8
		(1.999)			(93.2)
PbHCl	1.828	2.518		93.7	
$PbCl_2$		2.494			99.3
PbH_4	1.739		109.5		
	(1.805)		(109.5)		
PbH_3F	1.723	2.020	115.0	103.1	
	(1.795)	(2.001)	(113.2)	(105.4)	
PbH_2F_2	1.704	1.988	127.8	106.0	102.3
	(1.789)	(1.977)	(120.2)	(108.1)	(103.1)
$PbHF_3$	1.685	1.952		114.7	103.8
	(1.768)	(1.955)		(113.7)	(104.9)
PbF_4		1.924			109.5
		(1.936)			(109.5)
PbH_3Cl	1.723	2.466	114.2	104.2	
PbH_2Cl_2	1.709	2.429	122.3	106.8	105.4
$PbHCl_3$	1.704	2.399		112.3	106.5
$PbCl_4$		2.381			109.5

[a] Distances in Å, angles in deg. Results using the nonrelativistic Pb pseudopotential are given in parentheses. All other data have been obtained with the quasirelativistic pseudopotential.

Our results provide new insights. We have performed ab initio calculations, using both quasirelativistic and nonrelativistic pseudopotentials, on the structures and thermodynamics of a series of halogenated lead hydrides and alkyl lead compounds R_nPbX_{4-n} (R = H, CH_3; X = F, Cl; n = 0–4) and R_nPbX_{2-n} (n = 0–2). Data for R = CH_3, X = H are also provided for comparison. Energies for various isodesmic and other reactions are used to investigate the relative stabilities of these compounds. The Reed/Weinhold natural bond orbital analysis (NBO)[12] is employed to study the electronic origin of the observed thermodynamic and structural effects. Preliminary results for R = CH_3 and X = F have already been communicated.[13]

II. Computational Details

Hartree–Fock geometry optimizations, harmonic frequency calculations, and single-point calculations including electron correlation corrections at various levels of theory (MP2, MP4, QCISD(T))[14] at the

(1) (a) Cotton, F. A.; Wilkinson, G. *Advanced Inorganic Chemistry*, 5th ed.; Wiley: New York, 1988. (b) Greenwood, N. N.; Earnshaw, A. *Chemistry of the Elements*; Pergamon Press: Oxford, 1984. (c) Huheey, J. G. *Inorganic Chemistry: Principles of Structures and Reactiity*, 3rd ed.; Harper and Row: New York, 1983.

(2) (a) Harrison, P. G. In *Comprehensive Coordination Chemistry*; Wilkinson, G., Ed.; Pergamon Press: Oxford, 1987; Vol. 3, pp 183–235. (b) Harrison, P. G. In *Comprehensive Organometallic Chemistry*; Wilkinson, G., Stone, F. G. A., Abel, E. W., Eds.; Pergamon Press: Oxford, 1982; Vol. 1. (c) Aylett, B. J. *Organometallic Compounds*, 4th ed., Vol. I. Part 2 (Goups IV and V); Chapman and Hall: London, 1979.

(3) Brooker, S.; Buijink, J.-K.; Edelmann, F. T. *Organometallics* **1991**, *10*, 25.

(4) (a) Cf. ref 2a, pp 153–182, and ref 2b, pp 725–754 (Tl). (b) Cf. ref 2a; also see: Harrison, P. G. In *Comprehensive Organometallic Chemistry*, Wilkinson, G., Stone, F. G. A., Abel, E. W., Eds.; Pergamon Press: Oxford, 1982; Vol. 2, (Sn). (c) Cf. ref 2a, pp 153–182, and ref 2b, pp 683–724 (In).

(5) Sidgwick, N. V. *The Chemical Elements and Their Compounds*; Clarendon Press: Oxford, 1950; Vol, 1, p 287.

(6) Drago, R. S. *J. Phys. Chem.* **1958**, *62*, 353.

(7) Electrons in the vicinity of nuclei with large charge Z may exhibit velocities approaching considerable fractions of the velocity of light c (e.g., $v/c > 0.5$ for a 1s electron in mercury). In such cases the Schrödinger equation (which implies an infinite velocity of light) has to be replaced by expressions that take the finite velocity of light into account (e.g., the Dirac equation). The differences between data calculated with the correct finite value of c and calculations implying $c = \infty$ are defined as relativistic effects. A more detailed recent discussion may be found in: Baerends, E. J.; Schwarz, W. H. E.; Schwerdtfeger, P.; Snijders, J. G. *J. Phys. B: At. Mol. Opt. Phys.* **1990**, *23*, 3225. For excellent reviews of the influence of relativistic effects in chemistry, cf., e.g.: (a) Pyykkö, P. *Chem. Rev.* **1988**, *88*, 563. (b) Pyykkö, P.; Desclaux, J. P. *Acc. Chem. Res.* **1979**, *12*, 276. (c) Pitzer, K. S. *Acc. Chem. Res.* **1979**, *12*, 271. (d) Schwarz, W. H. E. In *Theoretical Models of Chemical Bonding*, Maksic, B., Ed.; Springer: Berlin, 1990; Vol. 2, p 593.

(8) Kutzelnigg, W. *Phys. Scr.* **1987**, *36*, 416. For recent reviews of relativistic pseudopotential calculations, see e.g.: Christiansen, P. A.; Ermler, W. C.; Pitzer, K. S. *Annu. Rev. Phys. Chem.* **1985**, *36*, 407. Balasubramanian, K.; Pitzer, K. S. *Adv. Chem. Phys.* **1987**, *67*, 287.

(9) See, e.g.: Ziegler, T. *Chem. Rev.* **1991**, *91*, 651.

(10) Schwerdtfeger, P.; Boyd, P. D. W.; Bowmaker, G. A.; Mack, H. G.; Oberhammer, H. *J. Am. Chem. Soc.* **1989**, *111*, 15.

(11) Schwerdtfeger, P.; Heath, G. A.; Dolg, M.; Bennett, M. A. *J. Am. Chem. Soc.* **1992**, *114*, 7518.

(12) (a) Reed, A. E.; Weinstock, R. B.; Weinhold, F. *J. Chem. Phys.* **1985**, *83*, 735. (b) Reed, A. E.; Weinhold, F. *J. Chem. Phys.* **1985**, *83*, 1736. (c) Reed, A. E.; Curtiss, L. A.; Weinhold, F. *Chem. Rev.* **1988**, *88*, 899.

(13) Kaupp, M.; Schleyer, P. v. R. *Angew. Chem.* **1992**, *104*, 1240. Kaupp, M.; Schleyer, P. v. R. *Angew. Chem., Int. Ed. Engl.* **1992**, *31*, 1224.

(14) (a) Explanations of standard levels of theory including Møller–Plesset perturbation theory may be found in: Hehre, W. J.; Radom, L.; Schleyer, P. v.R.; Pople, J. A. *Ab Initio Molecular Orbital Theory*; Wiley: New York, 1986. (b) For the QCISD(T) method see: Pople, J. A.; Head-Gordon, M.; Raghavachari, K. *J. Chem. Phys.* **1987**, *87*, 5968. Paldus, J.; Cizek, J.; Jeziorski, B. *J. Chem. Phys.* **1989**, *90*, 4356; **1990**, *93*, 1485. Raghavachari, K.; Head-Gordon, M.; Pople, J. A. *J. Chem. Phys.* **1990**, *93*, 1486.

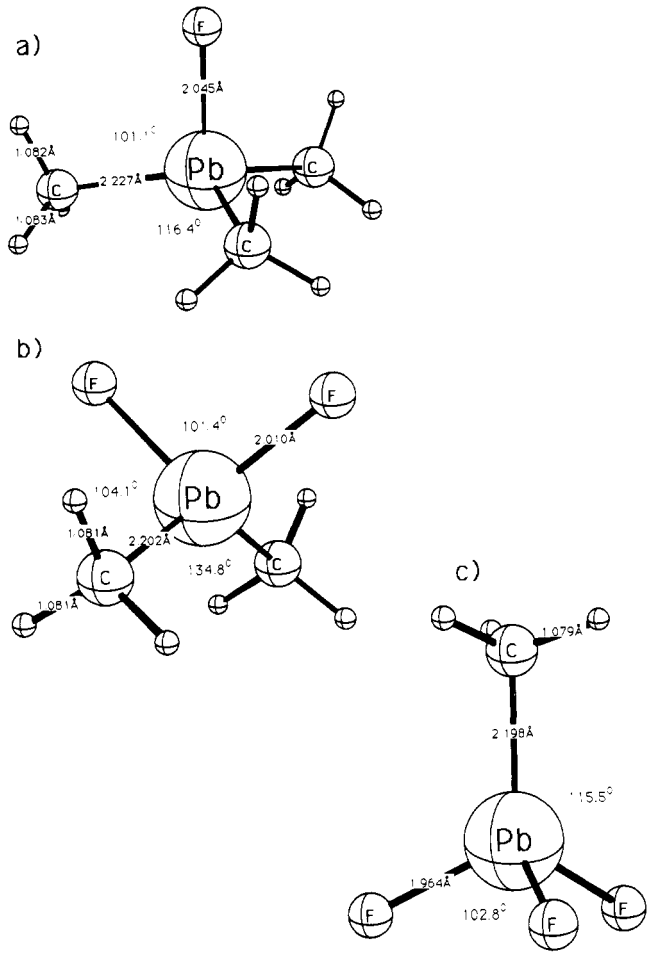

Figure 1. HF-optimized geometries for $(CH_3)_nPbF_{4-n}$ (n = 1–3): (a) $(CH_3)_3PbF$ (C_3), (b) $(CH_3)_2PbF_2$ (C_{2v}), (c) CH_3PbF_3 (C_{3v}).

HF-optimized geometries have been carried out with the Gaussian 90 program package[15] (if not stated otherwise, MP4 calculations include all single, double, triple, and quadruple substitutions of the reference determinant: MP4SDTQ[14a]). All electrons outside the pseudopotential cores were included in the active orbital space. As no analytical second derivatives involving pseudopotentials were available, harmonic frequencies and zero-point vibrational energy corrections have been calculated numerically from finite differences of the analytical first derivatives of the HF energies. The geometries have been fully optimized within T_d symmetry for PbX_4 and PbR_4, in C_{3v} symmetry for $RPbX_3$, $RPbH_3$, and H_3PbX, in C_3 symmetry for $(CH_3)_3PbX$, in C_{2v} symmetry for R_2PbX_2, PbX_2, and R_2Pb, and in C_s symmetry for RPbX. The harmonic frequency analyses confirm all of these structures to be minima on the corresponding potential energy surfaces.

A quasirelativistic and a nonrelativistic 4-valence-electron pseudopotential have been employed for lead.[16] Quasirelativistic multielectron-fit pseudopotentials have also been employed for C, Si, Sn (4-valence-electron description)[17] and for F and Cl (7-valence-electron description).[18a] For all nonhydrogen atoms 4s4p-valence basis sets[16,17,18b] in a 31/31 contraction have been augmented by one set of d-type polarization functions.[19] A diffuse sp set[18b] was added for F and Cl. Dunning and Hay's [4s1p]/(2s1p) hydrogen basis set[20] was used. The zero-point vibrational energy corrections for the methyl-substituted species were computed without polarization and diffuse functions at the geometries obtained with these unpolarized basis sets.

Molecular spin–orbit (SO) coupling is expected to be small for closed-shell species near their equilibrium geometries[10,11,21] and has not been considered. The experimental atomic SO splitting for the $Pb(^3P)$ ground state (24.4 kcal/mol)[22] is used for the thermochemistry of reactions involving atomic lead.

The Hartree–Fock wave functions of several species have been analyzed by natural bond orbital analysis,[12] involving natural atomic orbital (NAO) populations, strictly localized natural bond orbitals (NBO), and natural localized molecular orbitals (NLMO). For discussions of these methods, see ref 12. The Reed/Weinhold NAO/NBO/NLMO analysis is available as a part of the Gaussian 90 program package.[15]

Table II. HF-Optimized Geometries of Some Methyllead Compounds[a]

	Pb–C	Pb–X	C–Pb–C	C–Pb–X	X–Pb–X
$(CH_3)_2Pb$	2.323		93.0		
CH_3PbF	2.300	2.062		92.9	
CH_3PbH	2.321	1.835		93.1	
$(CH_3)_4Pb$	2.248		109.5		
$(CH_3)_3PbF$	2.227	2.045	116.4	101.1	
$(CH_3)_2PbF_2$	2.202	2.010	134.8	104.1	101.4
CH_3PbF_3	2.198	1.964		115.5	102.8
$(CH_3)_3PbH$	2.250	1.753	110.0	109.0	
$(CH_3)_2PbH_2$	2.244	1.748	110.5	109.5	108.4
CH_3PbH_3	2.242	1.744		110.1	108.9

[a] Distances in Å, angles in deg.

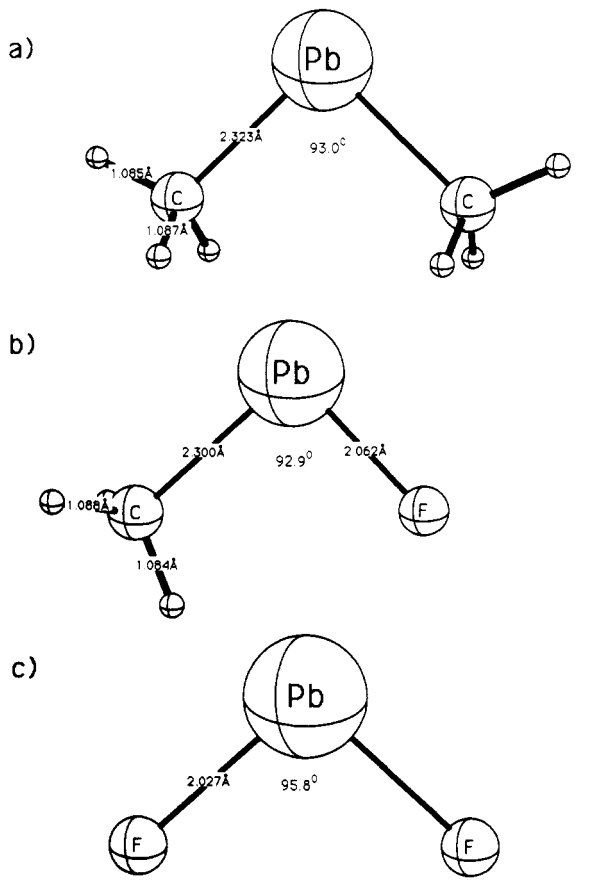

Figure 2. HF-optimized geometries for $(CH_3)_nPbF_{2-n}$ (n = 0–2): (a) $(CH_3)_2Pb$ (C_{2v}), (b) CH_3PbF (C_s), (c) PbF_2 (C_{2v}).

(15) Gaussian 90; Revision F: Frisch, M. J.; Head-Gordon, M.; Trucks, G. W.; Foresman, J. B.; Schlegel, H. B.; Raghavachari, K.; Robb, M.; Binkley, J. S.; Gonzalez, C.; DeFrees, D. J.; Fox, D. J.; Whiteside, R. A.; Seeger, R.; Melius, C. F.; Baker, J.; Kahn, L. R.; Stewart, J. J. P.; Topiol, S.; Pople, J. A. Gaussian, Inc.: Pittsburgh PA, 1990.

(16) Küchle, W.; Dolg, M.; Stoll, H.; Preuss, H. *Mol. Phys.* **1991**, *74*, 1245. Owing to program limitations, the g-projector (l = 3) of the semilocal lead pseudopotentials had to be used as a local term and was subtracted from the terms up to l = 2.

(17) Küchle, W.; Bergner, A.; Dolg, M.; Stoll, H.; Preuss, H., to be published.

(18) (a) Dolg, M., Ph.D. Thesis, University of Stuttgart, 1989. (b) Kaupp, M.; Schleyer, P.v.R.; Stoll, H.; Preuss, H. *J. Am. Chem. Soc.* **1991**, *113*, 6012.

(19) *Gaussian Basis Sets of Molecular Calculations*; Huzinaga, S., Ed.; Elsevier: New York, 1984.

(20) Dunning, T. H.; Hay, H. In *Methods of Electronic Structure Theory* (*Modern Theoretical Chemistry*, Vol. 3); Schaefer, H. F. III, Ed.; Plenum Press: New York, 1977; p 1 ff.

(21) (a) Schwerdtfeger, P. *Phys. Scr.* **1987**, *36*, 453. (b) Pitzer, K. *Int. J. Quantum Chem.* **1984**, *25*, 131.

(22) Moore, C. E. *Atomic Energy Levels*, Circular 467; National Bureau of Standards: Washington, DC, 1958.

Table III. Comparison with Some Experimental and Previous ab Initio Structural Data[a]

species	Pb–X	X–Pb–X angle	method[b]
PbF_2	2.027	95.8	this work, QRPP/HF
	1.999	93.2	this work, NRPP/HF
	2.018	95.8	QRPP/HF[c]
	1.983	94.3	NRPP/HF[c]
	2.047	96.7	QRPP/MP2[c]
	2.014	95.4	NRPP/MP2[c]
	2.036	96.5	PP/HF[d]
	2.03	97.8	exp (GED)[e]
$PbCl_2$	2.494	99.3	this work, QRPP/HF
	2.484	100.5	QRPP/HF[d]
	2.46	101.4	exp[f]
PbF_4	1.924	(109.5)	this work, QRPP/HF
	1.936	(109.5)	this work, NRPP/HF
	1.928	(109.5)	QRPP/HF[c]
	1.932	(109.5)	NRPP/HF[c]
	1.972	(109.5)	QRPP/MP2[c]
	1.966	(109.5)	NRPP/MP2[c]
$PbCl_4$	2.381	(109.5)	this work, QRPP/HF
	2.43	(109.5)	exp[f]
$(CH_3)_4Pb$	2.248	(109.5)	this work, QRPP/HF
	2.247	(109.5)	P-rel/HF[g]
	2.238	(109.5)	exp (GED)[h]

[a] Distances in Å, angles in deg. Extensive comparisons for PbH_2 and PbH_4 are given in ref 22, including the lead pseudopotentials used in the present work. [b] The abbreviations used are: QRPP (quasirelativistic pseudopotential), NRPP (nonrelativistic pseudopotential), HF (Hartree–Fock), MP2 (Møller–Plesset perturbation theory), P-rel (all-electron calculation with perturbative treatment of relativistic effects), exp (experimental data), GED (gas-phase electron diffraction). [c] Cf. ref 11. [d] Nizam, M.; Bouteiller, Y.; Allavena, M. *J. Mol. Struct.* **1987**, *159*, 365. [e] Demidov, A. Y.; Gershikov, A. G.; Zasorin, E. Z.; Spiridonov, V. P. *Zh. Struct. Khim.* **1983**, *24*, 7. [f] Chase, M. W.; Curnutt, J. L.; Prophet, H.; McDonald, R. A.; Syverud, A. N. *J. Phys. Ref. Data* **1975**, *4*, 1. [g] Almlöf, J.; Faegri, K., Jr. *Theor. Chim. Acta* **1986**, *69*, 438. [h] Oyamada, T.; Lijima, T.; Kimura, M. *Bull. Chem. Soc.* **1971**, *44*, 2638.

III. Results

A. Geometries. The optimized $(CH_3)_nPbF_{4-n}$ (n = 1–3) geometries are shown in Figure 1 and those for the corresponding Pb^{II} species in Figure 2. Tables I and II give the most important geometry parameters for the complete set of divalent and tetravalent species. Data for some of the few available experimental or previous theoretical structures (for PbF_4, PbF_2, $PbCl_4$, $PbCl_2$, and $(CH_3)_4Pb$) are summarized in Table III (a comparison of calculations with the lead pseudopotentials used in this work[16] to other results for PbH_2 and PbH_4 is given in ref 23a). The calculated geometries for PbH_2, PbH_4, PbF_2, $PbCl_2$, and PbF_4 are in good agreement with previous quasirelativistic SCF-pseudopotential results. The geometry $(CH_3)_4Pb$ also agrees with previous quasirelativistic calculations and with experiment (see Table III for details). The experimental data available for $PbCl_2$ and $PbCl_4$ appear to be somewhat uncertain, but the discrepancies between calculated and experimental Pb–Cl bond lengths are less than 5 pm. The relativistic bond contractions obtained for X = H, F also agree with previous calculations. Valence correlation is expected to increase bond lengths to Pb by ca. 0.02–0.05 Å (cf. Table III),[11,23] whereas core-valence correlation may lead to a slight contraction.[23a]

All of the unsymmetrically substituted tetravalent species (n = 1–3), except for $(CH_3)_nPbH_{4-n}$, deviate substantially from the idealized tetrahedral geometries. This is particularly obvious in the methyl fluoride series (cf. Figure 1). Generally, the R–Pb–R angles are considerably larger than 109.5°, whereas the R–Pb–X and particularly the X–Pb–X (X = F, Cl) angles are smaller. The C–Pb–C angle in $(CH_3)_2PbF_2$ is almost 135°; the F–Pb–F angle is only ca. 101° (Figure 1b). Similarly, the PbC_3 moiety in $(CH_3)_3PbF$ approaches planarity (Figure 1a). It is not possible to compare these computed deformations directly with experimental structures of monomeric lead species. R_3PbX and R_2PbX_2 compounds usually are polymeric in the solid state, and no gas-phase structures are available.[2,24] Spectroscopic features indicate

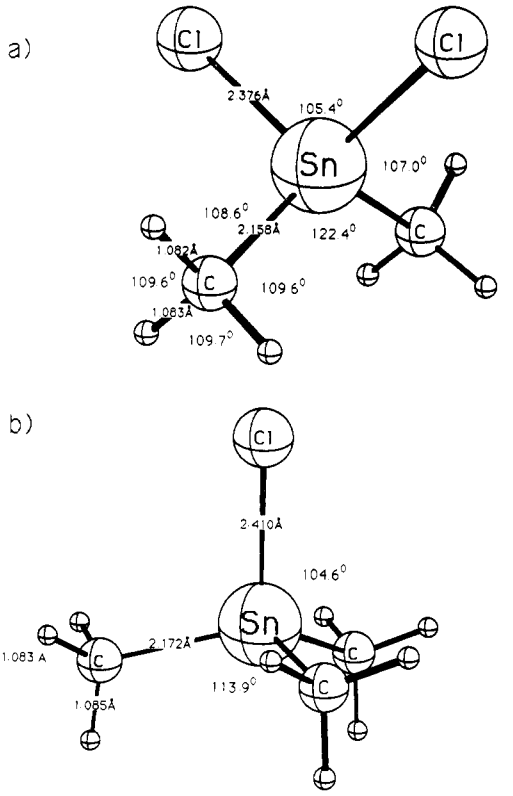

Figure 3. (a) HF-optimized geometry for $(CH_3)_2SnCl_2$ (C_{2v}); (b) optimized geometry for $(CH_3)_3SnCl$ (C_3).

that monomeric species are often present in solution, but no detailed structural data are known.[2] $RPbX_3$ species are even more difficult to study because of their instability. Nevertheless, our calculated structures may be related to polymeric arrangements found in the solid state: Ph_3PbX (X = Cl, Br) forms infinite $X–PbPh_3–X–PbPh_3–$ chains (with unsymmetrical bridges), in which almost planar $PbPh_3$ units are present (**1**).[25] Ph_2PbCl_2 exhibits a symmetrical chlorine bridging and octahedral coordination around lead, notably with a trans arrangement of the phenyl groups (**2**).[26] Very similar geometries also are found with other

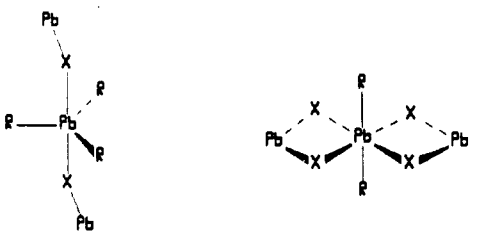

1 **2**

electronegative substituents, e.g., X = CH_3AlCl_3, N_3, NCO, NCS, OR, carboxylate, etc., as well as with other alkyl or aryl groups.[2] Thus, the polymeric solid-state structures are anticipated by the distortions we compute for the monomers.

More experimental information is available for tri- and dialkyltin halides. X-ray data indicate a wide range of structures from completely polymeric structures (akin to those described above for the lead species) to some apparently monomeric systems.[2,4b] In addition, some gas-phase geometries are available. In all reputedly monomeric R_3SnX[27] and R_2SnX_2[28] (X = halogen)

(23) (a) Dolg, M.; Küchle, W.; Stoll, H.; Preuss, H.; Schwerdtfeger, P. *Mol. Phys.* **1991**, *74*, 1265. (b) Schwerdtfeger, P.; Silberbach, H.; Miehlich, B. *J. Chem. Phys.* **1989**, *90*, 762.

(24) $Ph_3PbOSiPh$ is probably the only structurally characterized monomeric R_3PbX compound: Harrison, P. G.; King, T. J.; Richards, J. A.; Phillips, R. C. *J. Organomet. Chem.* **1976**, *116*, 307.

(25) Preut, H.; Huber, F. *Z. Anogr. Allg. Chem.* **1977**, *435*, 234.

(26) Mammi, M.; Busetti, V.; Del Pra, A. *Inorg. Chim. Acta* **1967**, *1*, 419.

Table IV. Calculated Energies (kcal/mol) for Isodesmic Reactions between Divalent and Tetravalent Lead Fluorohydrides

		nonrelativistic[a]	relativistic[b]	
	ZPE[c]	HF	HF	QCI[d]
(1) $PbH_4 + PbF_2 \rightarrow PbH_3F + PbHF$	−0.3	+13.4	+19.8	+21.4
(2) $PbH_4 + PbHF \rightarrow PbH_3F + PbH_2$	−0.6	+8.4	+14.9	+16.0
(3) $PbH_3F + PbF_2 \rightarrow PbH_2F_2 + PbHF$	−0.7	+14.1	+22.5	+23.0
(4) $PbH_3F + PbHF \rightarrow PbH_2F_2 + PbH_2$	−0.9	+9.1	+17.6	+17.7
(5) $PbH_2F_2 + PbF_2 \rightarrow PbHF_3 + PbHF$	−1.0	+16.8	+30.0	+28.8
(6) $PbH_2F_2 + PbHF \rightarrow PbHF_3 + PbH_2$	−1.2	+11.8	+25.1	+24.8
(7) $PbHF_3 + PbF_2 \rightarrow PbF_4 + PbHF$	−0.9	+23.3	+42.2	+40.6
(8) $PbHF_3 + PbHF \rightarrow PbF_4 + PbH_2$	−1.1	+18.3	+36.8	+35.2
(9) $PbH_4 + PbF_2 \rightarrow PbH_2F_2 + PbH_2$	−1.2	+22.5	+37.4	+39.0
(10) $PbH_3F + PbF_2 \rightarrow PbHF_3 + PbH_2$	−1.9	+25.9	+47.7	+47.9
(11) $PbH_2F_2 + PbF_2 \rightarrow PbF_4 + PbH_2$	−2.1	+35.1	+66.9	+65.3
(12) $PbH_4 + 2PbF_2 \rightarrow PbF_4 + 2PbH_2$	−3.3	+57.6	+104.0	+104.3

[a] Nonrelativistic lead pseudopotential. [b] Quasirelativistic lead pseudopotential. [c] SCF zero-point vibrational energy corrections with relativistic lead pseudopotential. [d] QCISD(T) energies.

Table V. Calculated Energies (kcal/mol) for Isodesmic Reactions between Divalent and Tetravalent Methyllead Fluorides[a]

	ZPE[b]	HF	MP4[c]
(1) $(CH_3)_4Pb + PbF_2 \rightarrow (CH_3)_3PbF + CH_3PbF$	−0.7	+8.9	+10.3[c]
(2) $(CH_3)_4Pb + CH_3PbF \rightarrow (CH_3)_3PbF + (CH_3)_2Pb$	−0.5	+9.8	+10.6[c]
(3) $(CH_3)_3PbF + PbF_2 \rightarrow (CH_3)_2PbF_2 + CH_3PbF$	−0.3	+15.1	+16.5
(4) $(CH_3)_3PbF + CH_3PbF \rightarrow (CH_3)_2PbF_2 + (CH_3)_2Pb$	−0.1	+16.0	+16.3
(5) $(CH_3)_2PbF_2 + PbF_2 \rightarrow CH_3PbF_3 + CH_3PbF$	−1.2	+29.1	+29.9
(6) $(CH_3)_2PbF_2 + CH_3PbF \rightarrow CH_3PbF_3 + (CH_3)_2Pb$	−1.0	+29.9	+30.0
(7) $CH_3PbF_3 + PbF_2 \rightarrow PbF_4 + CH_3PbF$	−1.2	+48.4	+47.4
(8) $CH_3PbF_3 + CH_3PbF \rightarrow PbF_4 + (CH_3)_2Pb$	−1.0	+49.3	+47.5
(9) $(CH_3)_4Pb + PbF_2 \rightarrow (CH_3)_2PbF_2 + (CH_3)_2Pb$	−0.8	+24.9	+26.4[c]
(10) $(CH_3)_3PbF + PbF_2 \rightarrow CH_3PbF_3 + (CH_3)_2Pb$	−1.3	+45.0	+46.3
(11) $(CH_3)_2PbF_2 + PbF_2 \rightarrow PbF_4 + (CH_3)_2Pb$	−2.2	+78.3	+77.3
(12) $(CH_3)_4Pb + 2PbF_2 \rightarrow PbF_4 + 2Pb(CH_3)_2$	−3.0	+103.2	+103.7[c]

[a] Quasirelativistic Pb pseudopotential used. [b] SCF zero-point vibrational energy corrections. [c] Reactions involving $(CH_3)_4Pb$ have been treated at the MP4SDQ level, all others at MP4SDTQ.

structures in the solid state, similar (albeit smaller) deviations from tetrahedral symmetry occur as those we compute for the lead systems. While such angle deviations have been ascribed to weak intermolecular interactions or steric hindrance, our results for monomers involving the small R = H, CH_3 groups and the large central atom Pb reveal that the underlying nature of these distortions is electronic, not steric.

The GED Cl–Sn–Cl and C–Sn–Cl angles in $(CH_3)_2SnCl_2$ were 107.5° (±3.9°) and 109.8° (±1.2°), respectively.[29] Our calculations (cf. Figure 3a) indicate far larger deviations from 109.5°. The GED structure for $(CH_3)_3SnCl$ exhibits 115° C–Sn–C and 103° C–Sn–Cl angles,[30] quite different from the ideal tetrahedral value, but in good agreement with our calculations (cf. Figure 3b). Note, that Tl^{III} compounds such as R_2TlX or $RTlX_2$ also exhibit significant deviations from the idealized 120° trigonal angles.[2,4,10]

The bond angle distortions are even larger when the substituents differ more in electronegativity. Figure 4 shows the remarkable structure resulting from replacement of the methyl groups in $(CH_3)_2PbF_2$ with more electropositive SiH_3 substituents. The Si–Pb–Si angle is larger than 140°! In contrast, the methyllead mixed hydrides $(CH_3)_nPbH_{4-n}$ (n = 1–3) do not deviate significantly from the ideal tetrahedral values (cf. Table II). This is consistent with the rather similar electronegativities of H and CH_3 (H, ca. 2.2; CH_3; ca. 2.5).

Both R–Pb and Pb–X bond distances decrease with increasing number of electronegative substituents, X. This agrees with the trends for the fluoromethane and fluorosilane series,[31,32] but

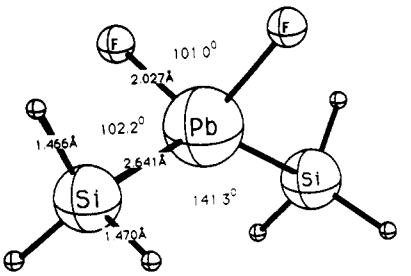

Figure 4. HF-optimized geometry for $(SiH_3)_2PbF_2$ (C_{2v}). The major geometry parameters obtained with the nonrelativistic lead pseudopotential are: R–PbF = 1.995 Å, R–PbSi = 2.713 Å; ∠FPbF = 101.5°, ∠FPbSi = 106.4°, ∠SiPbSi = 127.1°.

disagrees with the original formulation of Bent's isovalent rehybridization rule.[33] This rule does predict the decrease of the Pb–R distances correctly (less p-orbital contributions to the bond). However, isovalent rehybridization assuming orthogonal hybrids would require an increase in the Pb–X bond lengths (larger p-contributions to the bonds). See section IV.B for a discussion. Relatively large Pb–X distances in some R_2PbX_2 or R_3PbX X-ray structures[2] are probably due to the bridging of the ligand, X, and to the corresponding higher coordination numbers in the polymeric species. The Pb–C (and Pb–H) separations within the $(CH_3)_nPbH_{4-n}$ (n = 1–4) series do not differ much (cf. Table II).

As expected, all the divalent lead compounds favor bent structures with angles near 90° (cf. Figure 2, Table I). This agrees with available experimental and theoretical results (cf. Table III) and indicates that the lone pairs are stereochemically active[1a] (cf. section IV.E). As observed above for the tetravalent compounds,

(27) Calogero, S.; Ganis, P.; Peruzzo, V.; Tagliavini, G. *J. Organomet. Chem.* **1979**, *179*, 145. Bokii, N. G.; Zakharova, G. N.; Struchkov, Yu. T. *J. Struct. Chem.* (*Engl. Transl.*) **1970**, *11*, 828.
(28) Baxter, J. L.; Holt, E. M.; Zuckerman, J. J. *Organometallics* **1985**, *4*, 255.
(29) Fujii, H.; Kimura, M. *Bull. Chem. Soc. Jpn.* **1971**, *44*, 2643.
(30) Beagley, B.; McAloon, K.; Freeman, J. M. *Acta Crystallogr., Sect. B* **1974**, *B30*, 444.
(31) Reed, A. E.; Schleyer, P.v.R. *J. Am. Chem. Soc.* **1987**, *109*, 7362.
(32) Dixon, D. A. *J. Phys. Chem.* **1988**, *92*, 86.
(33) Bent, H. A. *Chem. Rev.* **1961**, *61*, 275.

Table VI. Calculated Energies (kcal/mol) for Isodesmic Reactions between Divalent and Tetravalent Lead Chlorohydrides[a]

	ZPE[b]	HF	QCI[c]
(1) $PbH_4 + PbCl_2 \rightarrow PbH_3Cl + PbHCl$	−0.3	+16.3	+17.8
(2) $PbH_4 + PbHCl \rightarrow PbH_3Cl + PbH_2$	−0.7	+15.5	+15.9
(3) $PbH_3Cl + PbCl_2 \rightarrow PbH_2Cl_2 + PbHCl$	−0.7	+20.4	+20.4
(4) $PbH_3Cl + PbHCl \rightarrow PbH_2Cl_2 + PbH_2$	−1.1	+19.6	+18.4
(5) $PbH_2Cl_2 + PbCl_2 \rightarrow PbHCl_3 + PbHCl$	−1.1	+25.2	+24.1
(6) $PbH_2Cl_2 + PbHCl \rightarrow PbHCl_3 + PbH_2$	−1.5	+24.4	+22.1
(7) $PbHCl_3 + PbCl_2 \rightarrow PbCl_4 + PbHCl$	−1.0	+29.2	+27.1
(8) $PbHCl_3 + PbHCl \rightarrow PbCl_4 + PbH_2$	−1.4	+28.4	+25.2
(9) $PbH_4 + PbCl_2 \rightarrow PbH_2Cl_2 + PbH_2$	−1.4	+35.9	+36.2
(10) $PbH_3Cl + PbCl_2 \rightarrow PbHCl_3 + PbH_2$	−2.2	+44.8	+42.5
(11) $PbH_2Cl_2 + PbCl_2 \rightarrow PbCl_4 + PbH_2$	−2.5	+53.6	+49.2
(12) $PbH_4 + 2PbCl_2 \rightarrow PbCl_4 + 2PbH_2$	−3.9	+89.5	+85.5

[a] Quasirelativistic Pb pseudopotential used. [b] SCF zero-point vibrational energy corrections. [c] QCISD(T) energies.

Table VII. Calculated Energies (kcal/mol) for Isodesmic Reactions between Tetravalent Lead Fluorohydrides

		nonrelativistic[a]	relativistic[b]	
	ZPE[c]	HF	HF	QCI[d]
(13) $3PbH_4 + PbF_4 \rightarrow 4PbH_3F$	+1.6	−14.1	−35.1	−29.7
(14) $2PbH_4 + PbHF_3 \rightarrow 3PbH_3F$	+1.0	−4.1	−13.1	−10.5
(15) $PbH_4 + PbH_2F_2 \rightarrow 2PbH_3F$	+0.4	−0.7	−2.8	−1.7

[a] Nonrelativistic lead pseudopotential. [b] Quasirelativistic lead pseudopotential. [c] SCF zero-point vibrational energy corrections with relativistic lead pseudopotential. [d] QCISD(T) energies.

Table VIII. Calculated Energies (kcal/mol) for Isodesmic Reactions between Tetravalent Methyllead Fluorides[a]

	ZPE[b]	HF	MP4[c]
(13) $3(CH_3)_4Pb + PbF_4 \rightarrow 4(CH_3)_3PbF$	+0.6	−65.8	−60.9[c]
(14) $2(CH_3)_4Pb + CH_3PbF_3 \rightarrow 3(CH_3)_3PbF$	+0.1	−26.3	−24.5[c]
(15) $(CH_3)_4Pb + (CH_3)_2PbF_2 \rightarrow 2(CH_3)_3PbF$	−0.4	−6.2	−5.5[c]

[a] Quasirelativistic Pb pseudopotential used. [b] SCF zero-point vibrational energy corrections. [c] MP4SDQ energies.

Table IX. Calculated Energies (kcal/mol) for Isodesmic Reactions between Tetravalent Lead Chlorohydrides[a]

	ZPE[b]	HF	QCI[c]
(13) $3PbH_4 + PbCl_4 \rightarrow 4PbH_3Cl$	+1.9	−25.9	−18.0
(14) $2PbH_4 + PbHCl_3 \rightarrow 3PbH_3Cl$	+1.2	−13.0	−8.7
(15) $PbH_4 + PbH_2Cl_2 \rightarrow 2PbH_3Cl$	+0.4	−4.1	−2.5

[a] Quasirelativistic Pb pseudopotential used. [b] SCF zero-point vibrational energy corrections. [c] QCISD(T) energies.

the bond distances usually decrease slightly upon substitution by electronegative groups, i.e., from R_2Pb to RPbX and from RPbX to PbX_2.

B. Relative Stabilities. Isodesmic and Group Separation Reactions. Isodesmic reactions allow the relative thermodynamic stabilities of a series of compounds to be evaluated.[14a] Electron correlation and (probably small) molecular spin–orbit (SO) contributions to the isodesmic reaction energies tend to cancel. Data for related sets of isodesmic reactions are given in Tables IV to XII. The energies of all these equations have been evaluated at the QCISD(T) or, where this is not practical, at the MP4SDTQ (or for $(CH_3)_4Pb$ MP4SDQ) levels. (Note that neither correlation nor zero-point vibrational energy corrections are very important; see Tables IV to XII). The best quasirelativistic pseudopotential QCI or MP4 values are generally given in the last column of each table.

Tables IV, V, and VI are ordered so that each equation describes similar reactions. Thus, eq 1 involves $PbH_4 + PbF_2$ in Table IV, $(CH_3)_4Pb + PbF_2$ in Table V, and $PbH_4 + PbCl_2$ in Table VI. Equations 1–11 show reactions between a tetravalent and a divalent lead compound with different substituents to give an new pair of tetravalent and divalent species in which the substituents have been exchanged. The number of electronegative substituents n(X) in the tetravalent species increases either by 1 (eqs 1–8) or by 2 (eqs 9–11) from the left to the right. For example, eq 1 in Table IV represents the transfer of one fluorine substituent from PbF_2 to PbH_4 to give PbH_3F (and PbHF). Equation 12 in Tables IV through VI is the sum of eqs 9 and 11 and corresponds to the extreme increase of n(X) from 0 to 4 (Δn(X) = 4).

Table X. Calculated Energies (kcal/mol) for Isodesmic Reactions between Tetravalent Methyllead Hydrides[a]

	ZPE[b]	HF	MP4[c]
(13) $3PbH_4 + (CH_3)_4Pb \rightarrow 4CH_3PbH_3$	+0.2	+0.9	+2.1
(14) $2PbH_4 + (CH_3)_3PbH \rightarrow 3CH_3PbH_3$	+0.0	+0.4	+1.2
(15) $PbH_4 + (CH_3)_2PbH_2 \rightarrow 2CH_3PbH_3$	+0.4	+0.1	+0.4

[a] Quasirelativistic Pb pseudopotential used. [b] SCF zero-point vibrational energy corrections. [c] MP4SDQ energies.

In general, eqs 1–11 in Tables IV to VI are strongly endothermic, particularly so in eqs 9–11 when the number of halogens n(X) in the tetravalent species increases by two (eqs 9–11). The destabilization of the tetravalent lead compounds by the electronegative substituents F or Cl is successive. The large endothermicity of eq 12 (more than 100 kcal/mol, Tables IV and V) demonstrates the remarkable destabilization that results when all hydrogens or methyl groups in R_4Pb are replaced by fluorines. With X = Cl eq 12 is still endothermic by ca. 85 kcal/mol (cf. Table VI).

The increase of the reaction energies from eq 1 to eq 8 and from eq 9 to eq 11 (Tables IV to VI) indicates cumulative effects. The isodesmic reactions are more endothermic when more halogens are already present in the educt. This is most pronounced by far in the $(CH_3)_nPbF_{4-n}$ series (Table V). For the lead fluorohydride set (Table IV), the ca. 5-kcal/mol differences between eqs 1 and 2, 3 and 4, 5 and 6, as well as 7 and 8, respectively, show the variation in stabilities of the divalent species (see below). The corresponding differences are much smaller for the methyllead hydrides (Table V) and for the lead chlorohydrides (Table VI).

Isodesmic group separation reactions, like the set of eqs 13 to 15 in Tables VII to X, provide a different criterion for relative stability of the substituted lead(IV) compounds. The reaction energies measure whether it is more favorable to have all geminal substituents X in one molecule (PbX_4, $RPbX_3$, or R_2PbX_2) or to have them separated (R_3PbX). Again, each numbered equation describes comparable reactions in all four tables, VII–X. Thus, eq 13 evaluates the stability of PbF_4 vs PbH_3F in Table VII, of PbF_4 vs $(CH_3)_3PbF$ in Table VIII, of $PbCl_4$ vs PbH_3Cl in Table IX, and of $(CH_3)_4Pb$ vs CH_3PbH_3 in Table X. Such isodesmic reactions have been used previously to define the nonadditive substituent interactions in first- and second-row compounds.[14a,31,32,34] Thus, reactions analogous to eqs 13, 14, and 15 are generally *endothermic* in the fluoromethane and to a lesser extent in the fluorosilane series; i.e., CH_nF_{4-n} and SiH_nF_{4-n} compounds are *stabilized* when more fluorines are present.[31-32] In contrast, the tetravalent lead compounds are strongly *destabilized* by multiple fluorine or chlorine substituents, as indicated by the considerable *exothermicity* of eqs 13, 14, and 15 in Tables VII to IX. Incremental geminal destabilization energies (i.e., destabilization per halogen substituent present)[31,34] can be obtained from the energies of eqs 13–15 in Tables VII to IX; in the lead fluorohydride series (Table VII), the increments are ca. 0.9, 3.5, and 7.4 kcal/mol for PbH_2F_2, $PbHF_3$, and PbF_4, respectively. The geminal destabilization is similar with the lead chlorohydrides (1.3, 2.9, and 6.0 kcal/mol for PbH_2Cl_2, $PbHCl_3$, and $PbCl_4$; cf. Table IX) but is considerably larger in the methyllead fluorides (2.8, 8.2, and 20.3 kcal/mol for $(CH_3)_2PbF_2$, CH_3PbF_3, and PbF_4; cf. Table VIII).

The very small energies for eqs 13–15 in Table X show that no significant geminal stabilization or destabilization results from substitution of methyl groups by hydrogen. However, note the different responses between the stabilities of methyl compounds and the corresponding hydrides when fluorine substituents are

(34) Dill, J. D.; Schleyer, P.v.R.; Pople, J. A. *J. Am. Chem. Soc.* **1976**, *98*, 1663. Dolbier, W. R.; Medinger, K. S.; Greenberg, A.; Liebman, J. F. *Tetrahedron* **1982**, *38*, 2415.

Table XI. Calculated Relative Stabilities (kcal/mol) of Methyllead Fluorides and Lead Fluorohydrides[a]

	ZPE[b]	HF	MP4[c]
(16) $PbH_4 + CH_3PbF_3 \rightarrow PbHF_3 + CH_3PbH_3$	−0.1	+10.1	+9.9
(17) $PbH_4 + (CH_3)_2PbF_2 \rightarrow PbH_2F_2 + (CH_3)_2PbH_2$	+0.2	+12.4	+12.5
(18) $PbH_4 + (CH_3)_3PbF \rightarrow PbH_3F + (CH_3)_3PbH$	+0.4	+8.1	+8.4

[a] Quasirelativistic Pb pseudopotential used. [b] SCF zero-point vibrational energy corrections. [c] MP4SDTQ energies.

Table XII. Calculated Energies (kcal/mol) for Isodesmic Reactions between Various Divalent Lead Compounds[a]

		nonrelativistic[a]	relativistic[b]	
	ZPE[c]	HF	HF	QCI
(19) $PbH_2 + PbF_2 \rightarrow 2PbHF$	−0.3	+5.0	+4.9	+5.1
(20) $(CH_3)_2Pb + PbF_2 \rightarrow 2CH_3PbF$	−0.2		−0.9	−0.1[d]
(21) $PbH_2 + PbCl_2 \rightarrow 2PbHCl$	+0.4		+0.8	+2.0
(22) $PbH_2 + (CH_3)_2Pb \rightarrow 2CH_3PbH$	+0.5		+0.3	+0.7[d]

[a] Nonrelativistic lead pseudopotential used. [b] Quasirelativistic lead pseudopotential used. [c] Zero-point vibrational energy corrections obtained with the quasirelativistic lead pseudopotential. [d] MP4SDTQ used for reactions involving methyl groups, otherwise QCISD(T).

Table XIII. Calculated Energies (kcal/mol) for 1,1-Elimination Reactions of Various Tetravalent Lead Compounds

		nonrelativistic[a]		relativistic[b]		
	ZPE[c]	HF	ΔE_R[d]	HF	MP4[e]	QCI[e]
(23) $PbF_4 \rightarrow PbF_2 + F_2$	−1.2	+149.3	−84.0	+65.3	+67.0	+64.5
(24) $PbHF_3 \rightarrow PbHF + F_2$	−2.1	+172.6	−65.6	+107.0	+108.8	+105.1
(25) $PbH_2F_2 \rightarrow PbH_2 + F_2$	−3.3	+184.4	−52.3	+132.1	+134.7	+129.9
(26) $CH_3PbF_3 \rightarrow CH_3PbF + F_2$	−2.4			+113.7	114.4	
(27) $(CH_3)_2PbF_2 \rightarrow (CH_3)_2Pb + F_2$	−3.4			+143.6	144.3	
(28) $PbHF_3 \rightarrow PbF_2 + HF$	+0.4	+4.7	−59.5	−54.8	−51.4	−51.0
(29) $PbH_2F_2 \rightarrow PbHF + HF$	−0.5	+21.5	−46.3	−24.8	−20.2	−20.8
(30) $PbH_3F \rightarrow PbH_2 + HF$	−1.5	+30.6	−37.7	−7.1	−1.6	−3.1
(31) $CH_3PbF_3 \rightarrow PbF_2 + CH_3F$	+0.2			−37.6	−28.5	
(32) $(CH_3)_2PbF_2 \rightarrow CH_3PbF + CH_3F$	−1.0			−8.5	+1.3	
(33) $(CH_3)_3PbF \rightarrow (CH_3)_2Pb + CH_3F$	−1.1			+7.5	+17.8	
(34) $PbH_2F_2 \rightarrow PbF_2 + H_2$	−2.6	+0.6	−40.2	−39.6	−43.7	−42.2
(35) $PbH_3F \rightarrow PbHF + H_2$	−3.3	+14.7	−31.8	−17.1	−19.7	−19.2
(36) $PbH_4 \rightarrow PbH_2 + H_2$	−3.9	+23.1	−25.3	−2.2	−2.9	−3.2
(37) $PbH_2Cl_2 \rightarrow PbCl_2 + H_2$	−2.5			−38.1	−39.5	−39.4
(38) $PbH_3Cl \rightarrow PbHCl + H_2$	−3.2			−17.7	−18.9	−19.0
(39) $(CH_3)_2PbH_2 \rightarrow (CH_3)_2Pb + H_2$	−4.2			−3.1	−5.7	
(40) $CH_3PbH_3 \rightarrow CH_3PbH + H_2$	−3.6			−2.5	−4.1	
(41) $(CH_3)_2PbF_2 \rightarrow PbF_2 + (CH_3)_2$	+0.4			−48.2	−44.1	
(42) $(CH_3)_3PbF \rightarrow CH_3PbF + (CH_3)_2$	+0.1			−33.1	−27.7	
(43) $(CH_3)_4Pb \rightarrow (CH_3)_2Pb + (CH_3)_2$	−0.4			−23.3	−17.9	
(44) $(CH_3)_3PbH \rightarrow CH_3PbH + (CH_3)_2$	−0.4			−23.3	−18.0	
(45) $(CH_3)_2PbH_2 \rightarrow PbH_2 + (CH_3)_2$	−1.1			−23.2	−15.7	
(46) $PbCl_4 \rightarrow PbCl_2 + Cl_2$	−0.8			+20.6	+25.3	+24.6
(47) $PbHCl_3 \rightarrow PbHCl + Cl_2$	−1.8			+49.8	+52.5	+51.7
(48) $PbH_2Cl_2 \rightarrow PbH_2 + Cl_2$	−3.3			+74.2	+74.7	+73.8
(49) $PbHCl_3 \rightarrow PbCl_2 + HCl$	−0.9			−33.4	−29.3	−29.4
(50) $PbH_2Cl_2 \rightarrow PbHCl + HCl$	−2.0			−8.3	−5.1	−5.3
(51) $PbH_3Cl \rightarrow PbH_2 + HCl$	−3.1			+11.4	+13.5	+13.1

[a] Nonrelativistic Pb pseudopotential. [b] Quasirelativistic Pb pseudopotential. [c] SCF zero-point vibrational energy corrections obtained with the quasirelativistic Pb pseudopotential. [d] Relativistic contribution to the reaction energy. [e] The MP4SDTQ and the QCISD(T) levels were used except for eq 43, which was treated at MP4SDQ.

present. Table XI probes the relative stabilities of the corresponding methyllead fluorides and the lead fluorohydrides (eqs 16–18). The endothermicity of these reactions indicates that the methyllead fluorides are more stable than the lead fluorohydrides (when the same number of fluorines are present). This effect already is significant when only one fluorine is present; $(CH_3)_3PbF$ is stabilized by ca. 8 kcal/mol vs PbH_3F (eq 18). This extra stabilization of $(CH_3)_3PbF$ contributes to the much larger geminal destabilization energies of eqs 13–15 in Table VIII than in Table VII (for the lead fluorohydrides). The large increase of the energies from eq 1 to eq 8 and from eq 9 to eq 11 in Table V (cf. above) is due to the larger geminal destabilization for the $(CH_3)_nPbF_{4-n}$ series compared to PbH_nX_{4-n} (X = F, Cl) or, better, to the stabilization of $(CH_3)_3PbF$ compared to PbH_3X.

The relative stabilities of various divalent species are compared in Table XII (eqs 19–22). Apparently, only the disproportionation energies of PbH_2, PbF_2, and PbHF (eq 19) are significant. This accounts for the small (ca 5 kcal/mol) variations in the isodesmic reaction energies involving the same tetravalent molecule but different divalent lead fluorohydrides (eqs 1 vs 2, 3 vs 4, 5 vs 6, and 7 vs 8 in Table IV). The effect of substitution on the stabilities of the other divalent species is even smaller (eqs 20, 21, 22 in Table XII).

Elimination Reactions. The 1,1-elimination reaction energies of tetravalent lead compounds are compared directly in Table XIII. Equations 23–51 evaluate the relative stabilities of compounds differing by two in their valency.[11] While the reactions are not isodesmic, the number of electron pairs is preserved. Thus, electron correlation corrections to the energies are moderate in magnitude, except for the ca. 5–10 kcal/mol effects in eqs 31 to 33 and 41 to 45, where methyl fluoride or ethane is eliminated. The available MP4SDTQ and QCISD(T) energies agree reasonably well.[11] The largest differences are observed for eqs 23 to 25, i.e., when F_2 (the theoretical description of which requires a good correlation

Table XIV. Fragmentation Energies, Average Pb–X Bond Energies, and Disproportionation Energies for Some PbX_2 and PbX_4 Species[a]

	PbH_2	PbH_4	$(CH_3)_2Pb$	$(CH_3)_4Pb$	PbF_2	PbF_4	$PbCl_2$	$PbCl_4$
ΔE_{fr}[b]								
SCF	75.5	158.6	36.7	80.1	122.8	149.1	114.0	146.1
MP2	100.5	201.1	86.2	167.8	209.1	311.2	161.8	
MP4SDTQ	106.4	210.1	82.9[c]	159.7[c]	200.9	290.7	156.3	223.8
QCISD(T)	107.4	211.1			196.0	283.9	155.6	222.1
+SO(Pb)[d]	83.0	186.7	58.5[c]	135.3[c]	171.6	259.5	131.2	197.7
+ZPE[e]	77.0	170.1	51.2[c]	116.5[c]	169.9	254.9	130.2	195.0
D_e(Pb–X)[f]	41.5	46.7	29.3[c]	33.8[c]	85.8	64.9	65.6	49.4
D_0(Pb–X)[f]	38.5	42.5	25.6[c]	29.1[c]	85.0	63.7	65.1	48.8
$\Delta E_{dispr.}$[d,g]	−21.8		−18.3[c]		+83.8		+64.7	
+ZPE[e]	−17.2		−14.1[c]		+85.0		+65.4	

[a] All energies in kcal/mol. Generally, single-point energies with the quasirelativistic lead pseudopotential at the HF-optimized geometries have been used. [b] Energies for the reactions $PbX_n \rightarrow Pb(^3P) + nX$. [c] MP4SDTQ without p-functions on hydrogen. [d] Experimental atomic SO splitting for Pb included (cf. ref 21). [e] Spin–orbit (Pb ^3P) and zero-point vibrational energy corrections included. [f] ΔE_{fr} divided by n. QCISD(T) results, except for X = CH_3. Atomic SO splitting for lead is included (experimental value of 24.4 kcal/mol from ref 21). Zero-point vibrational energy corrections included for D_0. [g] Disproportionation reaction 52: $2PbX_2 \rightarrow Pb(^3P) + PbX_4$. Levels as under footnote *f*.

treatment[35]) is involved. The equations in Table XIII have been grouped together according to the X_2, R_2, or RX species eliminated, as the stability of these elimination products strongly affects the reaction energies. As noted previously,[11] the elimination of the weakly bound F_2 is much less favorable than that of H_2 or HF.

The energies of the elimination reactions become more negative within a given section of Table XIII; i.e., they become less endothermic or more exothermic, when an increasing number of halogen substituents is present in the tetravalent lead compound. In some cases (eqs 31 to 33 or eqs 49 to 51) the energies even change from endothermic to exothermic when a larger number of halogens is present originally. This destabilization of the tetravalent species by electronegative substituents will alter the reactivity dramatically. As these trends are observed irrespective of the molecule eliminated (see Table XIII), *both Pb–R and Pb–X bonds must be weaker* when more halogens are present. However, CH_3 vs H substitution makes little difference (cf. eqs 36, 39, and 40, and eqs 43 to 45; these confirm the conclusions drawn from Table X).

Disproportionation and Fragmentation Energies. The calculated disproportionation energies (eq 52) are given at the bottom of

$$2PbX_2 \rightarrow Pb(^3P) + PbX_4 \qquad (52)$$

Table XIV for various species.

As our best energies for eq 52 with X = H, F are only slightly smaller than those obtained by Schwerdtfeger et al.[11] with larger valence basis sets, the trends probably are reliable. Equation 52 is exothermic both for PbH_4 and $(CH_3)_4Pb$. Hence, the thermodynamic stability of tetraalkyl lead compounds to reversal of eq 52 is comparable to that of PbH_4. This is similar to the thallium hydrides and thallium alkyls.[10] The high reactivity of the lead(IV) hydrides (e.g., PbH_4, $RPbH_3$, or R_2PbH_2 compared to R_4Pb^2) probably is not thermodynamic in origin. Disproportionation (eq 52) of $PbCl_2$ is slightly less unfavorable than that of PbF_2,[11] but still is significantly endothermic. The sign of the reaction energy for disproportionation depends on whether the average Pb–X bond in PbX_4 is weaker or stronger than that in PbX_2. Table XIV gives the calculated fragmentation energies ($PbX_4 \rightarrow Pb(^3P) + 4X$, and $PbX_2 \rightarrow Pb(^3P) + 2X$) and average bond energies for PbX_4 and PbX_2 (X = H, CH_3, F, Cl). Because of the relatively small valence basis sets used (restricted by the computational resources available for the methyl species), the correlation corrections and the dissociation energies are underestimated somewhat (cf. ref 11 for more accurate results with X = H, F). However, our calculations do show that the Pb–H and Pb–C bonds in PbH_4 and $(CH_3)_4Pb$ are slightly stronger than those in PbH_2 and $(CH_3)_2Pb$, respectively. On the other hand, the Pb–F and Pb–Cl bond energies in PbX_4 are only ca. 80% of those in the corresponding dihalides.[11]

(35) See, e.g.: Ahlrichs, R.; Lischka, H.; Zurawski, B.; Kutzelnigg, W. *J. Chem. Phys.* **1975**, *63*, 4685.

IV. Wave Function Analysis and a Qualitative Chemical Bonding Model

We now develop a general bonding model for the lead compounds. This must explain the following structural and thermodynamic generalizations which summarize the conclusions drawn from section III.

(1) Pb^{IV} compounds are strongly destabilized by electronegative substituents X (X = F, Cl). Both the Pb–R and the Pb–X bonds are weakened upon substitution by X = F and X = Cl.

(2) As a consequence of (1), the PbX bonds in PbX_4 (X = F, Cl) are weaker than those in PbX_2, but the Pb–R bonds in R_4Pb (R = H, CH_3) are slightly stronger than those in R_2Pb. However, *both* the Pb–R and the Pb–X bonds in the tetravalent species are shorter than those in the divalent compounds.

(3) The bond angles in unsymmetrically substituted species R_nPbX_{4-n} (R = H, CH_3, SiH_3; X = F, Cl) deviate considerably from 109.5°. The X–Pb–X angles are smaller, but the R–Pb–R angles are significantly larger than the idealized tetrahedral values.

(4) Both Pb–R and Pb–X bonds in the R_nPbX_{4-n} (R = H, CH_3; X = F, Cl) series are shorter when more electronegative groups X are present.

(5) As implied by (1) and (4), the increasing thermodynamic *destabilization* of the lead(IV) compounds upon successive substitution by F or Cl is accompanied by a *shortening* of the bonds to lead.

A. Hybridization and Stability. As demonstrated in detail by Kutzelnigg,[36,37] the familiar concept of sp^n hybridization (n = 1, 2, 3), which is so useful for first-row compounds (e.g., in organic chemistry), may only be transferred to the heavier main group elements when the restriction of orthogonal hybrids is removed. Except for first-row compounds (in particular for carbon), the valence p-orbitals in general are significantly larger than the corresponding s-orbitals. Therefore, the relative p-orbital contributions to covalent bonding in compounds of heavier main group elements are generally smaller than expected from symmetry considerations and orthogonal hybrids. These "*hybridization* defects"[36,37] result in smaller sp^n ratios (e.g., the central atom p/s ratio n in a tetrahedral molecule like SiH_4[36] or PbH_4 may be much smaller than 3; see below). Only nonbonding electrons, when present, will occupy orbitals with predominant s-character, and the p-involvement of the bonding electrons will be larger[36,37] (cf. section IV.E). As ideal hybrids with s- and p-orbitals of similar radial extent are particularly suited to form strong covalent bonds, the relative size of the s- and p-orbitals obviously is an important criterion for bond strength.[36,37] We will show that these orbital-size considerations provide the key to an understanding of the destabilization of Pb^{IV} vs Pb^{II} compounds when electronegative substituents are present.

Kutzelnigg[36,37] discussed hybridization and localization by using the contributions from Mulliken atomic gross populations[38] to

(36) Kutzelnigg, W. *Angew. Chem.* **1984**, *96*, 262; *Angew. Chem., Int. Ed. Engl.* **1984**, *23*, 272.

(37) Kutzelnigg, W. THEOCHEM **1988**, *169*, 403.

Table XV. NPA/NLMO Analysis of Hybridization in Haloplumbanes[a]

	Pb–NPA populations			NPA charges			NPA/NLMO hybr[b]	
species	Pb(6s)	Pb(6p)	Pb, av hybr[c]	Q(Pb)	Q(H)	Q(X)	σPbH	σPbX
PbH_4								
R[d]	1.114	2.007	$sp^{1.80}d^{0.003}$	0.876	−0.219		1.80	
NR[d]	0.960	1.735	$sp^{1.81}d^{0.008}$	1.298	−0.324		1.81	
PbH_3F								
R[d]	1.064	1.410	$sp^{1.33}d^{0.005}$	1.520	−0.254	−0.757	1.24	2.54
NR[d]	0.864	1.223	$sp^{1.42}d^{0.012}$	1.903	−0.370	−0.794	1.34	2.11
PbH_2F_2								
R[d]	0.975	0.983	$sp^{1.01}d^{0.005}$	2.037	−0.264	−0.755	0.80	1.90
NR[d]	0.734	0.856	$sp^{1.17}d^{0.010}$	2.399	−0.400	−0.799	0.98	1.74
$PbHF_3$								
R[d]	0.793	0.723	$sp^{0.91}d^{0.005}$	2.478	−0.257	−0.740	0.55	1.29
NR[d]	0.552	0.618	$sp^{1.12}d^{0.010}$	2.820	−0.416	−0.801	0.73	1.41
PbF_4								
R[d]	0.538	0.574	$sp^{1.07}d^{0.008}$	2.884		−0.721		0.92[e]
NR[d]	0.312	0.472	$sp^{1.51}d^{0.030}$	3.206		−0.802		1.24[e]
PbH_3Cl	1.121	1.628	$sp^{1.453}d^{0.005}$	1.246	−0.223	−0.578	1.31	2.60
PbH_2Cl_2	1.105	1.363	$sp^{1.234}d^{0.006}$	1.526	−0.212	−0.551	0.93	1.91
$PbHCl_3$	1.055	1.197	$sp^{1.134}d^{0.007}$	1.741	−0.199	−0.514	0.67	1.33
$PbCl_4$	0.987	1.090	$sp^{1.104}d^{0.009}$	1.915		−0.479		0.91

[a] The SCF wave functions have been analyzed. If not stated otherwise, the quasirelativistic lead pseudopotential was employed. [b] p/s ratios of lead NPA contributions to σ-NLMOs. [c] Average hybridization at Pb, 6s:6p:6d NPA ratios. [d] Quasirelativistic (R) and nonrelativistic (NR) lead pseudopotential used. [e] Some π-bonding contributions lead to the observed, slightly higher, NPA s:p ratio (cf. ref 30 for the situation in CF_4).

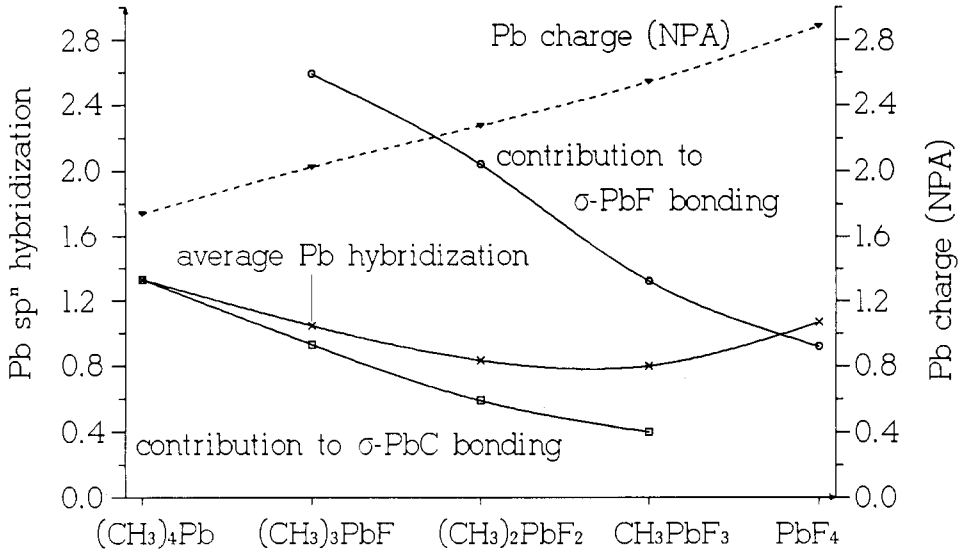

Figure 5. p/s ratios of lead NPA populations (for average population and lead NAO contributions to σ-bonding NLMOs) and lead NPA charges for the fluorinated methyllead series. The fact that the average curve and the σ-PbF NLMO curve do not coincide for PbF_4 is due to some π-type populations that contribute to the average value but not to the σ-NLMO. π contributions are also present for $MePbF_3$ (cf. ref 30 for the situation in CF_4).

localized molecular orbitals (employing the Foster–Boys criterion[39]). Our analysis is based on the "natural population analysis" (NPA) of Weinhold and co-workers combined with their "natural localized molecular orbitals" (NLMO).[12] The key step of the NPA/NLMO scheme is the transformation from the original nonorthogonal atomic basis into orthogonal "natural atomic orbitals" (NAO) via an "occupancy-weighted" Löwdin orthogonalization procedure.[12a] As no large overlap population has to be assigned to a particular atom, NPA is less basis-set dependent than the Mulliken analysis and more suitable to describe bonding situations with appreciable ionic character.[40] Table XV summarizes the results of the population/hybridization analyses for the Pb^{IV} fluoro- and chlorohydride series. Figure 5 shows the lead population p/s ratios and the net charges for the methyllead fluoride series.

The lead NPA charge Q(Pb) increases considerably, from ca. +0.9 in PbH_4 to ca +2.9 in PbF_4, and the average p/s population ratio decreases from 1.8 to 1.0 (Table XV). This indicates the strong electron-withdrawing power of the fluorine substituents (and is also observed for the chloro compounds to a lesser extent). The reported Mulliken charges[11] (obtained with relatively large valence basis sets) only change by ca. 0.3 electron from ca. +1.6 (PbH_4) to ca. +1.9 (PbF_4); the p/s ratio decreases from ca. 1.5 to ca. 1.0. The relatively small change in metal charge, typical of Mulliken populations when going to more ionic systems, is due to the equal distribution of the overlap populations.[40] However, the differences between the two methods do not affect the qualitative observation of a charge increase on Pb and of a decrease in the valence population p/s ratio from PbH_4 to PbF_4.

What is the relation between the increasing metal charge and the decreasing lead 6p/6s population ratio? The spin–orbit averaged experimental energies[22] to promote a 6s-electron to a 6p-orbital are ca. 176 kcal/mol in the ground state of Pb^+, ca. 206 kcal/mol in Pb^{2+}, and ca. 258 kcal/mol in Pb^{3+}. Thus, the sp-promotion gap within a series of related molecules is expected to become larger with increasing positive charge on lead. More importantly, the valence s-orbitals are expected to contract more dramatically in size than the p-orbitals, when the central atom becomes more positive. Thus, an increasing positive charge on lead due to electronegative substituents increases the size differences between 6s- and 6p-orbitals and makes efficient sp-hy-

(38) Mulliken, R. S. *J. Chem. Phys.* **1955**, *23*, 1833, 1841, 2338, 2343.
(39) Foster, J. M.; Boys, S. F. *Rev. Mod. Phys.* **1963**, *35*, 457.
(40) For a comparison of NPA and the Mulliken population analysis, cf. ref 12a.

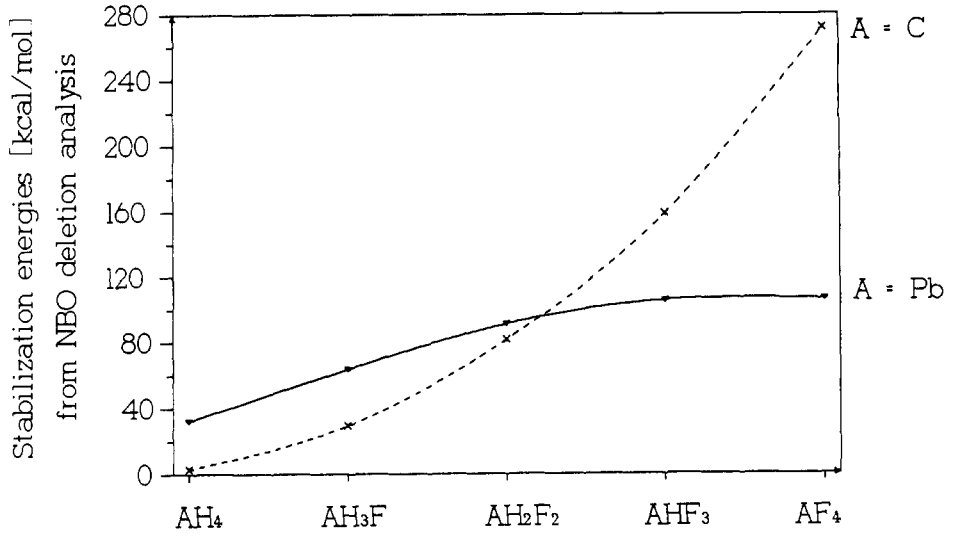

Figure 6. Comparison of delocalization contributions to the energies of fluoromethanes and fluoroplumbanes. All "antibonding" and "Rydberg-type" natural bond orbitals have been deleted from the Fock matrix in the NBO basis (cf. ref 12). The energy has then been recalculated (nonvariationally) by performing a single SCF cycle with the truncated Fock matrix. The difference to the full-variationally obtained energy is plotted.

bridization less favorable. This conclusion may be restated differently: *Ionic bonds to electronegative substituents deplete the lead p-orbitals more than the s-orbitals. The valence density remaining for covalent bonding therefore has large s-character. This precludes efficient directional bonding and leads to a weakening of the covalent bonds in lead(IV) compounds when electronegative substituents (e.g., X = F, Cl) are present.*

Even for PbH_4, the p-contributions to bonding are much smaller than expected from symmetry considerations and orthogonal hybrids.[36,37] The NPA hybridization of $sp^{1.8}$ is well below the sp^3 valence configuration in neutral Pb^{IV} and also below the sp^2 excited configuration in Pb^{1+} (cf. Table XV). The observed NPA hybridization of ca. $sp^{1.1}$ in PbF_4 differs greatly from sp^3 or the 100% p-population for the p-excited state in Pb^{3+} (indeed, the p/s ratio of the lead NPA contributions to the Pb–F bonding NLMOs is only 0.9. Small hyperconjugative π-bonding contributions increase the average p/s ratio slightly, as observed previously for CF_4;[31] cf. section IV.B). Obviously, bonding models based on orthogonal hybrids are inappropriate for these heavy main group compounds. The tetravalent lead compounds studied here exhibit relatively small "localization defects"[36,37] (generally more than 99.8% of the electron density may be assigned to a single "Lewis structure" given by strictly localized "natural bond orbitals"; cf. section IV.B) but dramatic "*hybridization* defects".[36,37] Peters probably made the first implicit use of nonorthogonal hybrids in his early qualitative MO discussion of bonding in the fluoromethane series.[41] Note that the concept of orthogonal hybrids also fails with relatively ionic first-row species like BeH_2.[31]

The traditional term "inert pair effect"[5] implies that the s-orbitals are too low in energy to participate in bonding. While this describes the situation in the Pb^{II} compounds (cf. section IV.E), it does not explain why the Pb^{IV} species are destabilized. The discussion above makes clear that the weak bonds (e.g., in PbF_4 vs PbF_2) are not due to the unavailability of s-orbitals for bonding. Instead, the lead 6p-orbitals are too large to be accessible for efficient sp^3 hybridization in the tetravalent species. Thus, the preference of inorganic lead compounds to occur as Pb^{II} species is due to the *hybridization defects*[36,37] in the corresponding Pb^{IV} derivatives. More covalent bonds involve a smaller positive metal charge and smaller hybridization defects. Hence, organolead chemistry is dominated by Pb^{IV}.

Electrostatic repulsions between the negatively charged substituents also could contribute to the destabilization of the substituted systems (cf. NPA charges in Table XV). However, if this Coulomb repulsion effect were significant, one would expect larger angles between the electronegative substituents and not the smaller ones resulting from "isovalent" rehybridization. Moreover, one would expect a significant destabilization of PbF_2 vs PbH_2. This does not seem to be the case.

Table XVI. Decomposition of Group Separation Reaction Energies (kcal/mol)[a]

	E_{HF}	E_L	E_D
(13) $3PbH_4 + PbF_4 \rightarrow 4PbH_3F$	−35.1	+17.0	−52.1
(14) $2PbH_4 + PbHF_3 \rightarrow 3PbH_3F$	−13.1	+8.2	−21.3
(15) $PbH_4 + PbH_2F_2 \rightarrow 2PbH_3F$	−2.8	+1.2	−4.0

[a] The Hartree–Fock energy E_{HF} (cf. Table VII) is decomposed by NBO Fock-matrix deletion analysis (ref 24) into a contribution from the Lewis structure E_L and contributions from delocalization E_D.

B. Negative $n(F) \rightarrow \sigma^*(PbH, PbF)$ Hyperconjugation versus Geminal $\sigma PbH \rightarrow \sigma^*(PbH, PbF)$ Hyperconjugation. Why are polyfluoromethanes stabilized compared to CH_4 or CH_3F?[31,32,41] As Reed and Schleyer showed by "natural bond orbital" (NBO) analysis, negative hyperconjugation involving $n(F) \rightarrow \sigma^*(AH, AF)$ interactions are responsible for the stabilization of many polyfluorinated first-row compounds (e.g., A = C).[31] Obviously, this stabilization by delocalization (i.e., by deviations from ideal Lewis structures) should be less pronounced with the heavier central atom lead.

Figure 6 compares the energy increases observed for the fluorinated methanes and plumbanes, when all low-occupied natural bond orbitals (corresponding to deviations from the ideal Lewis structures) are deleted from the NBO Fock matrix.[31,42] Obviously, methane exhibits almost no delocalization stabilization, but the slope of the line from CH_4 to CF_4 increases dramatically. On the other hand, PbH_4 and PbH_3F are stabilized much more than CH_4 and CH_3F, respectively. However, the increase of the delocalization contributions (i.e., the NBO Fock-matrix deletion energies) from PbH_4 to PbF_4 is much less than for the carbon analogues and the slope of the line decreases.

As a result, the delocalization interactions favor the monosubstituted derivative, PbH_3F, which is important in the group separation reactions of the lead fluorohydrides (eqs 13–15 in Table VII; cf. section III.B). This is shown in Table XVI, where the results of the NBO Fock-matrix deletion analyses (Figure 6) are used to decompose the energies of eqs 13 to 15 (E_{HF}) into a contribution from the Lewis structure (E_L) and a delocalization contribution (E_D). Obviously, the Lewis energies E_L favor the left side of the equations, whereas the delocalization energies E_D are responsible for the exothermicity of these reactions. This is

(41) Peters, D. J. *J. Chem. Phys.* **1963**, *38*, 561.

(42) Reed. A. E.; Schleyer, P.v.R. *Inorg. Chem.* **1988**, *27*, 3969.

Table XVII. Decomposition of 1,1-Elimination Reaction Energies (kcal/mol)[a]

	E_{HF}	E_L	E_D
(34) $PbH_2F_2 \rightarrow PbF_2 + H_2$	−39.6	−105.3	+65.7
(35) $PbH_3F \rightarrow PbHF + H_2$	−17.1	−66.8	+49.7
(36) $PbH_4 \rightarrow PbH_2 + H_2$	−2.2	−32.2	+30.0

[a] The Hartree–Fock energy E_{HF} (cf. Table XIII) is decomposed by NBO Fock-matrix deletion analysis (ref 24) into a contribution from the Lewis structure E_L and contributions from delocalization E_D.

completely opposite to the situation for the analogous fluoromethanes, where the delocalization contributions E_D are responsible for the endothermicity of the group separation reactions and for the nonadditive stabilization by geminal fluorine substitution.[31]

Second-order perturbation theory analysis of the Fock matrix based on strictly localized natural bond orbitals[12,31] indicates that the most important deviations from ideal Lewis structures in the lead compounds are different in character from those noted previously for first- and second-row fluorohydrides.[31] While n(F) → σ^*(AF, AH) negative hyperconjugation is the dominant contribution in the fluoromethanes and the fluorosilanes (A = C, Si),[31] geminal σPbH → σ^*(PbF, PbH) interactions yield the largest perturbational energy expressions in the lead fluorohydride series (we previously noted the appreciable size of such geminal compared to vicinal hyperconjugation in the heavy group 14 ethane congeners[43]). Even though these important energy contributions increase upon successive substitution of hydrogen by fluorine (for example, the second-order energies for individual σPbH → σ^*PbH interactions increase from ca. 4 kcal/mol in PbH_4 to ca. 15 kcal/mol in PbH_2F_2), *their number decreases* (the number of σPbH donor orbitals decreases and σPbF bonds are considerably worse donors for geminal hyperconjugation). The less-than-linear increase of delocalization contributions in the lead fluorohydride series (cf. Figure 6) results. The individual second-order n(F) → σ^*(PbH, PbF) negative hyperconjugation energies generally are only in the 2–5-kcal/mol range. The σPbC bonds in the methyllead fluorides are better donors in geminal hyperconjugation than the σPbH bonds in the lead fluorohydrides. This explains why $(CH_3)_3PbF$ is stabilized more than PbH_3F (cf. Table XI), and why the group separation reactions (eqs 13–15) are considerably more exothermic for the methyllead fluorides (Table VIII) than for the lead fluorohydrides (Table VII).

However, the hyperconjugation interactions are not the origin of the destabilization of Pb^{IV} vs Pb^{II} when electronegative substituents are present. This conclusion is shown clearly by decomposition of the 1,1-elimination reaction energies (cf. Table XIII and discussion in section III.B) into the Lewis structure and the delocalization contributions E_L and E_D. A few examples are given in Table XVII. Indeed, the delocalization interactions *stabilize* Pb^{IV} vs Pb^{II} and *reduce* the energy increase from eq 34 to eq 36 (Table XVII). The same trend holds true for other sets of equations in Table XIII (e.g., eqs 23 through 25 or eqs 28 through 30). Thus, the destabilization of the polysubstituted lead(IV) fluorohydrides in group separation reactions by geminal hyperconjugation (Table XVI) should not be confused with the destabilization of lead(IV) vs lead(II) compounds by electronegative substituents. The latter effect is due to the *hybridization defects*[36,37] discussed in the preceding section.

C. Hybridization and Structural Trends. The direction of the deviations of the bond angles in the unsymmetrically substituted species R_nPbF_{4-n} (n = 1–3) from 109.5° (cf. section III.A) agrees with Bent's isovalent rehybridization rule.[33,41] Smaller angles between the more electronegative substituents (F, Cl) indicate more p-character in these bonds; the larger angles between the less electronegative groups imply more s-character. This explanation is supported by the NPA/NLMO hybridization analysis (see last two columns in Table XV). In all cases H_nPbX_{4-n} (n = 1–3; X = F, Cl), the p/s ratio of the lead NPA contributions to the Pb–X bonding NLMOs is about twice as large as that in the Pb–H bonding NLMOs (the same holds true for the Pb–C and Pb–F bonds in $(CH_3)_nPbF_{4-n}$; cf. Figure 5).

Why are the deviations from idealized tetrahedral angles so large for the lead compounds? While the effect is increased by relativistic contributions (cf. section IV.D), there are other reasons why such angle distortions usually are much smaller with first- or second-row central atoms. Reed and Schleyer showed that n(F) → σ^*(CH, CF) negative hyperconjugation partially cancels the structural deformations in fluoromethanes caused by the inductive substituent effects.[31] When the delocalization contributions are "removed" via an NBO Fock-matrix deletion procedure[12] (see above), the bond angles resulting for the H_nCF_{4-n} series (n = 1–3) are very similar to those given in Table I for the lead fluorohydrides. For example, the HF/6-31G* H–C–H angle of CH_2F_2 is 112.5°.[31] After deletion of all "antibonding" or "Rydberg-type"[12] NBOs from the Fock-matrix, an angle of 122.6° is obtained,[31] in good agreement with the nonrelativistically optimized H–Pb–H angle of 120.2° in PbH_2F_2 (cf. Table I). Owing to less favorable orbital overlap, negative hyperconjugation of halogen lone pairs into antibonding σ^*PbH or σ^*PbF orbitals is much smaller with lead (cf. above). Thus, the angular distortions due to "rehybridization" are not compensated by hyperconjugation (indeed, preliminary calculations indicate that the delocalization interactions enhance the deviations from 109.5° angles in the lead(IV) derivatives), but these distortions are amplified by relativistic effects (cf. section IV.D). The description of the unsymmetrically substituted species as ion pairs would be the limiting case; $(CH_3)_3PbF$, e.g., could be taken approximately as a complex of planar $(CH_3)_3Pb^+$ with F^-. This extreme ionic point of view seems to be adequate for many species R_2TlX, which feature linear R_2Tl^+ ions.[1,2,4]

Why are *both* Pb–R and Pb–X bonds shorter when more electronegative substituents X are present? As shown in Table XV, the NPA/NLMO hybridizations satisfy Bent's rule only insofar as the relative distribution of the lead 6p population into the Pb–X and Pb–H σ-bonding NLMOs is concerned. The p/s ratios and the average lead NPA hybridizations reflect the increasing depletion of the high-lying 6p-orbitals when the number of electronegative substituents n(X) is increased (the 6s populations also decrease, but less dramatically). Thus, all bonds exhibit more s-character and shorten when the positive charge on lead is increased. One can also speak of an electrostatic contraction effect,[44] e.g., Pb^{3+} is smaller than Pb^{1+}. As the large 6s-contributions to the bonds also render orbital overlap, important for covalent bonding, less efficient, *related effects are responsible for both shortening and weakening of the bonds* upon substitution by F or Cl.

D. The Influence of Relativistic Effects. Relativistic Effects on Geometries. Relativistic effects may change the bond lengths in lead compounds considerably.[7] Much less is known about the influence of such effects on bond angles.[7a] The main relativistic effects on the geometries of the lead fluorohydrides may be deduced from Table I by comparing the structures calculated with a nonrelativistic lead pseudopotential[16] (values in parentheses) and those obtained using the quasirelativistic pseudopotential.

The deviations from tetrahedral bond angles (cf. sections III.A and IV.C) in PbH_nF_{4-n} (n = 1–3) are less dramatic in the nonrelativistic calculations (cf. Table I. Note the ca. 8° relativistic increase of the H–Pb–H angle in PbH_2F_2). The R–Pb–R bond angle expansions, particularly the 14° widening of the Si–Pb–Si angle in $(SiH_3)_2PbF_2$ (cf. Figure 4), are the largest relativistic effects on bond angles yet noted.[7a] One may expect even larger changes in other hypothetical systems, such as, e.g., $(PbH_3)_2PbF_2$. In contrast, we confirm that relativistic effects on the bond angles of the divalent species (Table I) are small.[7a,11,23]

The NPA/NLMO charges, populations, and hybridization ratios for the lead fluorohydrides, obtained with the nonrelativistic and the quasirelativistic lead pseudopotential, are compared in Table XV. Relativistic effects decrease the metal charge Q(Pb), but also decrease the p/s ratio of the average valence population

(43) Schleyer, P.v.R.; Kaupp, M.; Hampel, F.; Bremer, M.; Mislow, K. *J. Am. Chem. Soc.* **1992**, *114*, 6791.

(44) Cf. ref 30 and further references given therein.

Table XVIII. NPA/NLMO Analysis of Hybridization in Some Divalent Lead Compounds[a]

	Pb–NPA populations			NPA charges			NPA/NLMO hybr[b]		
species	Pb(6s)	Pb(6p)	Pb, av hybr[c]	Q(Pb)	Q(H)	Q(X)	σPbH	σPbX	LP(Pb)
PbH_2									
R[d]	1.791	1.426	$sp^{0.796}d^{0.003}$	0.781	−0.390		10.10		0.19
NR[d]	1.701	1.421	$sp^{0.835}d^{0.007}$	0.872	−0.436		6.61		0.29
PbHF									
R[d]	1.829	0.855	$sp^{0.467}d^{0.004}$	1.311	−0.481	−0.830	11.99	13.24	0.12
NR[d]	1.730	0.899	$sp^{0.520}d^{0.005}$	1.363	−0.517	−0.846	7.51	7.97	0.20
PbF_2									
R[d]	1.852	0.453	$sp^{0.245}d^{0.003}$	1.691		−0.845		12.62	0.09
NR[d]	1.743	0.530	$sp^{0.304}d^{0.007}$	1.721		−0.860		7.98	0.16
PbHCl									
R[d]	1.848	1.020	$sp^{0.552}d^{0.004}$	1.128	−0.440	−0.688	12.04	17.93	0.12
$PbCl_2$									
R[d]	1.895	0.706	$sp^{0.372}d^{0.006}$	1.393		−0.697		20.35	0.07

[a] The SCF wave functions have been analyzed. [b] p/s ratios of lead NPA contributions to NLMOs. [c] Average hybridization at Pb, 6s:6p:6d NPA ratios. [d] Quasirelativistic (R) or nonrelativistic (NR) lead pseudopotential used.

on lead, owing to the relativistic contraction of the 6s-orbital. Generally, the p/s ratio of the lead NPA contributions to the σPbH bonds is smaller at the relativistic level (cf. next to last column in Table XV). The 6p/6s ratio for the σPbF NLMOs (last column) either decreases less pronounced (e.g., in $PbHF_3$) or increases in the relativistic calculations (PbH_3F and PbH_2F_2). Thus, the more covalent PbH bonds, which already exhibit larger lead 6s-contributions, are influenced more strongly by the relativistic contraction of the 6s-orbital than the more ionic PbF bonds. Hence, the preferred direction of the available lead p-orbital population into the bonds to the more electronegative substituents (Bent's rule[33]) is increased by relativistic effects. This results in larger deviations from idealized tetrahedral bond angles. The molecules studied here are ideal examples of how relativistic effects may affect the angular distribution of valence density and thus change bond angles.

Consistent with previous findings,[7,11,23] the Pb–H bonds in the tetravalent species are shortened considerably by relativistic effects (cf. Table I; note the much smaller change in the divalent species). In contrast, the Pb–F bonds lengthen (by ca. 1.9 and 1.1 pm for PbH_3F and PbH_2F_2) or shorten slightly (by ca. 0.3 and 1.2 pm for $PbHF_3$ and PbF_4). The Pb–Si bond $(SiH_3)_2PbF_2$ (cf. Figure 4) shortens by ca. 7 pm, and the Pb–F bond lengthens (by ca. 3 pm).

Many factors contribute to relativistic bond length changes, and the detailed interpretation may depend on the computational method employed.[45] A simple qualitative argument may suffice to rationalize the observed effects for the well-localized σ-bonds encountered here. Appreciably covalent bonds, which have significant contributions from the lead 6s-orbital (e.g., the Pb–H bonds), will experience significant relativistic bond shortening (cf. Table I). The bond contraction is accompanied by a decrease of the p/s hybridization ratio for these bonds (cf. Table XV). More ionic bonds with larger 6p-contributions (e.g., the Pb–F bonds) contract less. Owing to redistribution of p-character from the Pb–H into the Pb–F bonds (cf. above and Table XV), the Pb–F bonds may even expand slightly (cf. PbH_3F, PbH_2F_2; Table I). Smaller relativistic effects on fluorine bond lengths compared to hydrogen bond lengths have been noted for all 6th-period elements from Au to Bi.[11]

Relativistic Effects on Stabilities. In general, relativistic effects have been found to destabilize bonds to lead.[7,11,23] However, the bonds in Pb^{IV} species are weakened more dramatically than bonds in Pb^{II} compounds. Therefore, the stability balance of lead(IV) vs lead(II) is shifted in favor of lead(II) by relativistic effects.[7,11,23] This is confirmed by the energies of the 1,1-elimination reactions calculated with a quasirelativistic and with a nonrelativistic lead pseudopotential (cf. eqs 23 to 25, 28 to 30, and 34 to 36, second and fourth column in Table XIII; the third column gives the net relativistic contributions ΔE_R to the reaction energies). The relativistic destabilization of Pb^{IV} vs Pb^{II} (or of Tl^{III} vs Tl^{I}, or Bi^{V} vs Bi^{III}[11]) has been attributed to the considerably larger central atom s-orbital contributions to the bonds in the higher-valent species.[7,11] The larger the s-contributions to the bond, the larger the destabilization of the bond due to the relativistic contraction of the s-orbitals.

We find that this relativistic destabilization of tetravalent versus divalent lead compounds depends on the substituents. Thus, the relativistic contributions ΔE_R to the energies of the elimination reactions are larger when more fluorines are present originally (cf. the decrease in ΔE_R from eq 23 to 25, eq 28 to 30, and eq 34 to 36 in Table XIII). Isodesmic SCF reaction energies obtained with the nonrelativistic lead pseudopotential for the H_nPbF_{4-n} series are given in Tables IV and VII (second column). Equations 1–12 (Table IV) are much less endothermic at the nonrelativistic level. This shows that the destabilization of the lead(IV) species by fluorine substituents is increased by relativistic effects. The group separation reactions (eqs 13–15 in Table VII) are considerably less than half as exothermic at the nonrelativistic level, whereas the energy of eq 18 (i.e., the relative stability of PbH_2, PbHF, and PbF_2, Table XII) is not affected by relativistic effects.

The participation of the lead 6s-orbitals in bonding may be used to rationalize the significant relativistic contributions to the destabilization of tetravalent lead compounds by fluorine substitution. As the charge increase on lead from PbH_4 to PbF_4 is accompanied by a decrease of the p/s ratio of the remaining lead valence population (cf. Table XV and section IV.A), the relative s-contributions to the bonds increase along the series $PbH_4 < PbH_3F < PbH_2F_2 < PbHF_3 < PbF_4$. This leads to an increase in the relativistic destabilization of the bonds. Related interpretations have been used before, e.g., to explain the increase in the relativistic contributions to the reaction energies, $TlX_3 \rightarrow TlX + X_2$, with $X = H < I < Br < Cl < F$.[11] Indeed, the relation between the s-character of the central-atom hybrids and the relativistic destabilization is completely in line with our proposed bonding model (section IV.A).

E. Bonding in the Pb^{II} Species. As indicated by NPA/NLMO hybridization analysis (Table XVIII), the *lone pairs* in the Pb^{II} species R_2Pb, RPbX, and PbX_2 are largely comprised of 6s-orbitals, slightly polarized by small 6p-contributions. In contrast, the lead NPA contributions to the Pb–R and Pb–X *bonds* exhibit large p-character. As discussed in detail by Kutzelnigg,[37] this does not contradict the notion of a "sterochemically active lone pair."[1a] The "backside lobes" (with predominant p-character) of the (nonorthogonal) hybrids involved in bonding of the ligands extend into the region of the lone pairs. These p-contributions may lead to a displacement of the "lone-pair" density away from the bond regions and "create" sterochemically active lone pairs.[37]

As observed for the Pb^{IV} species, the lead NPA charges in the Pb^{II} derivatives increase and the average p/s ratio of the valence populations decrease, when H is replaced by F or Cl (cf. Table XVIII). A shortening of all bonds results (cf. Tables I and II and section III.A). Note that the average hybridization of the valence population on lead in all of these Pb^{II} species differs

(45) Schwarz, W. H. E. *Phys. Scr.* **1987**, *36*, 403.

considerably from the sp^2 suggested by isovalent hybridization with orthogonal hybrids (Table XVIII).

Relativistic effects decrease the ionicity and further decrease the p/s ratios of the average lead valence populations (Table XVIII). Because of the large 6p-character of the bonds, relativistic effects have only a small effect on Pb–F and Pb–H bond lengths in PbF_2, PbHF, and PbH_2 (cf. Tables I and II). As there is no significant hybridization with the 6s-orbital, relativity does not influence the bond angles in these divalent species (in agreement with previous studies[7a,11,23]).

V. Conclusions

Ab initio pseudopotential calculations delineate the remarkable thermodynamic destabilization of lead(IV) compounds by electronegative substituents. Based on population analyses of the molecular wave functions, a simple qualitative explanation is proposed. Electronegative substituents increase the metal charge and increase the difference in the radial extensions of the 6s- and 6p-orbitals. Consequently, the contribution of 6p-orbitals to covalent bonding in lead(IV) species becomes increasingly unfavorable when more electronegative substituents are present. While the bonds are *weakened* by these "*hybridization defects*",[36,37] the increasing s-character actually leads to *shorter* bond lengths.

The traditional "inert-pair effect"[5] implies that the s-orbitals of the central atom are too low in energy to participate in bonding. In contrast, our proposed concept emphasizes the differences in the sizes (radial extensions) of s- and p-orbitals. When these size differences increase, sp^n hybridization becomes increasingly unfavorable, and the covalent bonds will be weaker. This agrees with Kutzelnigg's general description of bonding in compounds of the heavier main group elements.[36,37] By increasing the differences in the radial extensions of the s- and p-orbitals, 6th-row relativistic effects also contribute to a destabilization of the higher valence state. Because of the increased relative 6s-contributions to the bonds in the electronegatively substituted species, the relativistic destabilization is larger in these cases.

The deviations of the molecular wave functions from "ideal Lewis structures", i.e., the delocalizations, are considerably different in character for the lead(IV) species than for the homologous carbon compounds. While $n(F) \rightarrow \sigma^*(CH, CF)$ negative hyperconjugation is the dominant contribution in fluoromethanes,[31] geminal $\sigma PbH \rightarrow \sigma^*(PbH, PbF)$ hyperconjugation is more important than negative hyperconjugation for the fluoroplumbanes(IV). As a result, geminal fluorosubstitution is stabilizing for fluoromethanes but destabilizing for lead(IV) fluorohydrides. This preference for geminal over vicinal hyperconjugation may be of general importance for compounds of heavy group 14 elements.

How general are the simple concepts we propose? They certainly will pertain to tin and, to a lesser extent, to germanium chemistry, even though the thermodynamics of the disproportionation or elimination reactions (section III.B) will differ quantitatively. Carbon behaves somewhat differently, because negative hyperconjugation stabilizes compounds with multiple geminal fluorine substituents.[31] Extension of our concept to group 13 is straightforward (while R_2TlX species are more stable than R_3Tl in the condensed phase, this may be due to ion pair $R_2Tl^+X^-$ formation[2,4]). Note that the reaction $TlH_3 + 3TlF \rightarrow TlF_3 + 3TlH$ ($\Delta n(X) = 3$) is endothermic by ca. 87 kcal/mol.[11] Hence, the destabilization by fluorine substituents in Tl^{III} vs Tl^{I} and in Pb^{IV} vs Pb^{II} is comparable. Remarkably, the disproportionation reaction, $2BiX_3 \rightarrow BiX + BiX_5$, is endothermic even with X = H, although this is less so than with X = F.[11] Thus, the apparent influence of electronegative substituents may not be as large in group 15 as in groups 13 and 14.

The angles of polysubstituted compounds R_nPbX_{4-n} (R = CH_3, H, SiH_3; X = F, Cl; n = 1–3) deviate substantially from 109.5°. This is due to inductive substituent effects, which are virtually uncompensated by negative hyperconjugation (in contrast to the corresponding carbon and silicon compounds[31]). The deviation is increased by relativistic effects. The computational findings may be related to a wealth of structural data for unsymmetrically substituted organolead and organotin species R_3MX and R_2MX_2, both in the solid state and in the gas phase.[2,4,24-30]

Our study pertains to the thermodynamics and structures in the gas phase. Lattice energies of Pb^{II} and Pb^{IV} species or the aggregation of the free metal[11] will contribute to the relative stabilities of different oxidation states in condensed phases. Many questions are still open. Why are organolead(IV) hydrides much more reactive than tetraalkyl or tetraaryl compounds (PbH_4 is unknown)? Why can lead tetraacetate be handled without difficulty, in spite of its strong oxidation power, whereas $PbCl_4$ is an elusive species? While further investigations are required, our proposed conceptual model should help to interpret and to understand heavy element chemistry more fully.

Acknowledgment. This work was supported by the Deutsche Forschungsgemeinschaft, the Fonds der Chemischen Industrie, the Stiftung Volkswagenwerk, and Convex Computer Corporation. M.K. acknowledges a Kekulé scholarship by the Fonds der Chemischen Industrie. We thank Professor H. Stoll (Stuttgart) for simulating discussions and for providing as yet unpublished pseudopotentials and basis sets of the Stuttgart group.[17] We are grateful to Dr. P. Schwerdtfeger (Auckland) and Dr. M. Dolg (Stuttgart) for a preprint of ref 11. We also acknowledge helpful suggestions by Dr. A. Korkin (Erlangen).